EUROPEAN ORGANISATION FOR PARTICLE PHYSICS

CERN PPE/93-174
24 September 1993

Studies of Charged Particle Multiplicity in b Quark Events

The OPAL Collaboration

Abstract

Using the distance from the average primary vertex to reconstructed secondary vertices in jets, samples of events with b purity varying from about 13% to 89% have been selected. The charged particle multiplicity in the hemispheres opposite those containing these jets has been studied as a function of the b purity of the events. Extrapolating to 0% and 100% b purity, values of the hemisphere charged particle multiplicity in $Z^0 \to b\overline{b}$ events and in non-$b\overline{b}$ events have been measured to be

$$\bar{n}_{\mathrm{b}} = 11.71 \pm 0.03 \pm 0.18 \pm 0.21$$

$$\bar{n}_{\mathrm{udsc}} = 10.32 \pm 0.01 \pm 0.07 \pm 0.19.$$

The first error is statistical, the second systematic and the third is a common systematic error.
The difference in charged particle multiplicity between b quark events and light (u, d, s) quark events has been measured and found to be

$$\delta_{\mathrm{bl}} = 3.02 \pm 0.05 \pm 0.79.$$

The result is compared to the predictions of MLLA QCD calculations.
By studying the impact parameter distributions of charged particles in the hemispheres opposite these jets, the charged particle decay multiplicity of B hadrons from Z^0 decay, including particles from K^0_s and Λ decay, has been measured to be

$$\bar{n}^{\mathrm{B}} = 5.51 \pm 0.05 \pm 0.51.$$

From the mean momentum of these decay products and separately from the number of primary charged particles per b event, the average x_E of b flavoured hadrons has been measured to be

$$\langle x_E \rangle_{\mathrm{b}} = 0.693 \pm 0.003 \pm 0.030.$$

(Submitted to Zeitschrift für Physik C)

The OPAL Collaboration

R. Akers[16], G. Alexander[23], J. Allison[16], K.J. Anderson[9], S. Arcelli[2], A. Astbury[28], D. Axen[29], G. Azuelos[18,a], J.T.M. Baines[16], A.H. Ball[17], J. Banks[16], R.J. Barlow[16], S. Barnett[16], R. Bartoldus[3], J.R. Batley[5], G. Beaudoin[18], A. Beck[23], G.A. Beck[13], J. Becker[10], C. Beeston[16], T. Behnke[27], K.W. Bell[20], G. Bella[23], P. Bentkowski[18], P. Berlich[10], S. Bethke[11], O. Biebel[3], I.J. Bloodworth[1], P. Bock[11], B. Boden[3], H.M. Bosch[11], M. Boutemeur[18], H. Breuker[8,b], P. Bright-Thomas[25], R.M. Brown[20], A. Buijs[8], H.J. Burckhart[8], C. Burgard[27], P. Capiluppi[2], R.K. Carnegie[6], A.A. Carter[13], J.R. Carter[5], C.Y. Chang[17], D.G. Charlton[8], S.L. Chu[4], P.E.L. Clarke[15], J.C. Clayton[1], I. Cohen[23], J.E. Conboy[15], M. Cooper[22], M. Coupland[14], M. Cuffiani[2], S. Dado[22], G.M. Dallavalle[2], S. De Jong[13], L.A. del Pozo[5], H. Deng[17], A. Dieckmann[11], M. Dittmar[4], M.S. Dixit[7], E. do Couto e Silva[12], J.E. Duboscq[8], E. Duchovni[26], G. Duckeck[11], I.P. Duerdoth[16], D.J.P. Dumas[6], P.A. Elcombe[5], P.G. Estabrooks[6], E. Etzion[23], H.G. Evans[9], F. Fabbri[2], B. Fabbro[21], M. Fierro[2], M. Fincke-Keeler[28], H.M. Fischer[3], D.G. Fong[17], M. Foucher[17], A. Gaidot[21], J.W. Gary[4], J. Gascon[18], N.I. Geddes[20], C. Geich-Gimbel[3], S.W. Gensler[9], F.X. Gentit[21], G. Giacomelli[2], R. Giacomelli[2], V. Gibson[5], W.R. Gibson[13], J.D. Gillies[20], J. Goldberg[22], D.M. Gingrich[30,a], M.J. Goodrick[5], W. Gorn[4], C. Grandi[2], F.C. Grant[5], J. Hagemann[27], G.G. Hanson[12], M. Hansroul[8], C.K. Hargrove[7], P.F. Harrison[13], J. Hart[8], P.M. Hattersley[1], M. Hauschild[8], C.M. Hawkes[8], E. Heflin[4], R.J. Hemingway[6], G. Herten[10], R.D. Heuer[8], J.C. Hill[5], S.J. Hillier[8], T. Hilse[10], D.A. Hinshaw[18], J.D. Hobbs[8], P.R. Hobson[25], D. Hochman[26], R.J. Homer[1], A.K. Honma[28,a], R.E. Hughes-Jones[16], R. Humbert[10], P. Igo-Kemenes[11], H. Ihssen[11], D.C. Imrie[25], A.C. Janissen[6], A. Jawahery[17], P.W. Jeffreys[20], H. Jeremie[18], M. Jimack[1], M. Jones[29], R.W.L. Jones[8], P. Jovanovic[1], C. Jui[4], D. Karlen[6], K. Kawagoe[24], T. Kawamoto[24], R.K. Keeler[28], R.G. Kellogg[17], B.W. Kennedy[15], J. King[13], S. Kluth[5], T. Kobayashi[24], D.S. Koetke[8], T.P. Kokott[3], S. Komamiya[24], J.F. Kral[8], R. Kowalewski[8], J. von Krogh[11], J. Kroll[9], P. Kyberd[13], G.D. Lafferty[16], H. Lafoux[21], R. Lahmann[17], J. Lauber[8], J.G. Layter[4], P. Leblanc[18], A.M. Lee[31], E. Lefebvre[18], M.H. Lehto[15], D. Lellouch[26], C. Leroy[18], J. Letts[4], L. Levinson[26], S.L. Lloyd[13], F.K. Loebinger[16], J.M. Lorah[17], B. Lorazo[18], M.J. Losty[7], X.C. Lou[12], J. Ludwig[10], A. Luig[10], M. Mannelli[8], S. Marcellini[2], C. Markus[3], A.J. Martin[13], J.P. Martin[18], T. Mashimo[24], P. Mättig[3], U. Maur[3], J. McKenna[29], T.J. McMahon[1], J.R. McNutt[25], F. Meijers[8], D. Menszner[11], F.S. Merritt[9], H. Mes[7], A. Michelini[8], R.P. Middleton[20], G. Mikenberg[26], J. Mildenberger[6], D.J. Miller[15], R. Mir[12], W. Mohr[10], C. Moisan[18], A. Montanari[2], T. Mori[24], M. Morii[24], U. Müller[3], B. Nellen[3], H.H. Nguyen[9], S.W. O'Neale[1], F.G. Oakham[7], F. Odorici[2], H.O. Ogren[12], C.J. Oram[28,a], M.J. Oreglia[9], S. Orito[24], J.P. Pansart[21], B. Panzer-Steindel[8], P. Paschievici[26], G.N. Patrick[20], N. Paz-Jaoshvili[23], M.J. Pearce[1], P. Pfister[10], J.E. Pilcher[9], J. Pinfold[30], D. Pitman[28], D.E. Plane[8], P. Poffenberger[28], B. Poli[2], T.W. Pritchard[13], H. Przysiezniak[18], G. Quast[27], M.W. Redmond[8], D.L. Rees[8], G.E. Richards[16], M. Rison[5], S.A. Robins[5], D. Robinson[8], A. Rollnik[3], J.M. Roney[28], E. Ros[8], S. Rossberg[10], A.M. Rossi[2], M. Rosvick[28], P. Routenburg[30], K. Runge[10], O. Runolfsson[8], D.R. Rust[12], M. Sasaki[24], C. Sbarra[2], A.D. Schaile[26], O. Schaile[10], W. Schappert[6], F. Scharf[3], P. Scharff-Hansen[8], P. Schenk[4], B. Schmitt[3], H. von der Schmitt[11], M. Schröder[12], C. Schwick[27], J. Schwiening[3], W.G. Scott[20], M. Settles[12], T.G. Shears[5], B.C. Shen[4], C.H. Shepherd-Themistocleous[7], P. Sherwood[15], G.P. Siroli[2], A. Skillman[16], A. Skuja[17], A.M. Smith[8], T.J. Smith[28], G.A. Snow[17], R. Sobie[28], R.W. Springer[17], M. Sproston[20], A. Stahl[3], C. Stegmann[10], K. Stephens[16], J. Steuerer[28], R. Ströhmer[11], D. Strom[19], H. Takeda[24], T. Takeshita[24,c], S. Tarem[26], M. Tecchio[9], P. Teixeira-Dias[11],

N. Tesch[3], M.A. Thomson[15], E. Torrente-Lujan[22], S. Towers[28], G. Transtromer[25], N.J. Tresilian[16], T. Tsukamoto[24], M.F. Turner[8], D. Van den plas[18], R. Van Kooten[27], G.J. VanDalen[4], G. Vasseur[21], A. Wagner[27], D.L. Wagner[9], C. Wahl[10], C.P. Ward[5], D.R. Ward[5], P.M. Watkins[1], A.T. Watson[1], N.K. Watson[8], M. Weber[11], P. Weber[6], P.S. Wells[8], N. Wermes[3], M.A. Whalley[1], B. Wilkens[10], G.W. Wilson[4], J.A. Wilson[1], V-H. Winterer[10], T. Wlodek[26], G. Wolf[26], S. Wotton[11], T.R. Wyatt[16], R. Yaari[26], A. Yeaman[13], G. Yekutieli[26], M. Yurko[18], W. Zeuner[8], G.T. Zorn[17].

[1]School of Physics and Space Research, University of Birmingham, Birmingham, B15 2TT, UK
[2]Dipartimento di Fisica dell' Università di Bologna and INFN, Bologna, 40126, Italy
[3]Physikalisches Institut, Universität Bonn, D-5300 Bonn 1, Germany
[4]Department of Physics, University of California, Riverside, CA 92521 USA
[5]Cavendish Laboratory, Cambridge, CB3 0HE, UK
[6]Carleton University, Dept of Physics, Colonel By Drive, Ottawa, Ontario K1S 5B6, Canada
[7]Centre for Research in Particle Physics, Carleton University, Ottawa, Ontario K1S 5B6, Canada
[8]CERN, European Organisation for Particle Physics, 1211 Geneva 23, Switzerland
[9]Enrico Fermi Institute and Dept of Physics, University of Chicago, Chicago Illinois 60637, USA
[10]Fakultät für Physik, Albert Ludwigs Universität, D-7800 Freiburg, Germany
[11]Physikalisches Institut, Universität Heidelberg, Heidelberg, Germany
[12]Indiana University, Dept of Physics, Swain Hall West 117, Bloomington, Indiana 47405, USA
[13]Queen Mary and Westfield College, University of London, London, E1 4NS, UK
[14]Birkbeck College, London, WC1E 7HV, UK
[15]University College London, London, WC1E 6BT, UK
[16]Department of Physics, Schuster Laboratory, The University, Manchester, M13 9PL, UK
[17]Department of Physics, University of Maryland, College Park, Maryland 20742, USA
[18]Laboratoire de Physique Nucléaire, Université de Montréal, Montréal, Quebec, H3C 3J7, Canada
[19]University of Oregon, Dept of Physics, Eugene, Oregon 97403, USA
[20]Rutherford Appleton Laboratory, Chilton, Didcot, Oxfordshire, OX11 0QX, UK
[21]DAPNIA/SPP, Saclay, F-91191 Gif-sur-Yvette, France
[22]Department of Physics, Technion-Israel Institute of Technology, Haifa 32000, Israel
[23]Department of Physics and Astronomy, Tel Aviv University, Tel Aviv 69978, Israel
[24]International Centre for Elementary Particle Physics and Dept of Physics, University of Tokyo, Tokyo 113, and Kobe University, Kobe 657, Japan
[25]Brunel University, Uxbridge, Middlesex, UB8 3PH UK
[26]Particle Physics Department, Weizmann Institute of Science, Rehovot, 76100, Israel
[27]Universität Hamburg/DESY, II Inst für Experimental Physik, Notkestrasse 85, 22607 Hamburg, Germany
[28]University of Victoria, Dept of Physics, P O Box 3055, Victoria BC V8W 3P6, Canada
[29]University of British Columbia, Dept of Physics, Vancouver BC V6T 1Z1, Canada
[30]University of Alberta, Dept of Physics, Edmonton AB T6G 2N5, Canada
[31]Duke University, Dept of Physics, Durham, North Carolina 27708-0305, USA

[a]Also at TRIUMF, Vancouver, Canada V6T 2A3
[b]Now at MPI, München, Germany
[c]Also at Shinshu University, Matsumoto 390, Japan

1 Introduction

Heavy flavour and especially b quark physics is becoming an increasingly significant area of LEP physics. For many of the production and decay properties of b quarks, we rely at the moment on measurements taken at much lower energies around the $\Upsilon(4s)$ and from ad hoc fragmentation models. However, because of the relatively large mass of the b quark, the fragmentation of b quarks into B hadrons can to some extent be treated perturbatively in QCD. It is important to measure as many properties of B hadron production and decay as possible at LEP and where relevant to compare these with theory.

In this paper we report on a study of charged particle multiplicity in $Z^0 \to b\overline{b}$ decays. Precision tracking, including information from our silicon microvertex detector, was used to reconstruct secondary vertices in jets. Using the distance of these vertices from the average beam interaction point, samples of events with varying b purity were produced. The charged particle multiplicity and impact parameter distributions of the tracks in the hemispheres opposite those containing the reconstructed vertices were studied as a function of the b purity of the events. Results on the charged particle multiplicity in $Z^0 \to b\overline{b}$ and non-$b\overline{b}$ events separately are presented and compared with predictions from QCD. The charged particle multiplicity of b events is also separated into the primary (non-leading) component and that coming from B hadron decays. The results are then used to estimate the mean x_E of b flavoured hadrons in $Z^0 \to b\overline{b}$ events.

2 The OPAL Detector

A complete description of the OPAL detector can be found elsewhere[1, 2]. Only a brief description of the components particularly relevant to this analysis are included here. Tracking of charged particles is performed by the central detector which consists of a silicon microvertex detector, a precision vertex drift chamber, a large volume jet chamber and chambers measuring the z-coordinate[1] of tracks as they leave the jet chamber. Excluding the silicon microvertex detector, the system allows detection of charged particles over 98% of the full solid angle with a track finding efficiency close to 100% for tracks in the region $|\cos\theta| < 0.92$. The central detector is positioned inside a solenoid coil that provides a uniform magnetic field of 0.435 T. The coil is surrounded by a time-of-flight counter array and a lead glass electromagnetic calorimeter with presampler. Outside the electromagnetic calorimeter is the return yoke of the magnet, which is instrumented as a hadron calorimeter and is surrounded by muon chambers.

The silicon microvertex detector[2] is crucial to this analysis. It consists of two concentric arrays of silicon strip detectors at radii of 6.1 cm and 7.5 cm surrounding a 5.3 cm radius beryllium beampipe. Each silicon wafer has 629 readout strips with a pitch of 50μm. The detector has an active length of 18 cm, giving 2 layer coverage for $|\cos\theta| < 0.76$. Within this acceptance, each layer covers approximately 90% of the solid angle with an efficiency for reconstructing a hit within the fiducial region of the silicon wafers of 97%. The detectors provide $r\phi$ hit coordinates with an intrinsic precision of better than 6μm but this is limited to about 10μm by alignment uncertainties. When combined with angle and curvature information provided by the other

[1]The OPAL coordinate system is defined with positive z along the electron beam direction with θ and ϕ being the polar and azimuthal angles, respectively.

central detector components, the impact parameter resolution for $Z^0 \to \mu^+\mu^-$ and $Z^0 \to e^+e^-$ events is 18μm.

3 Event Selection and Monte Carlo Simulation

This analysis is based on about 17.3 pb^{-1} of data recorded in 1992 at the Z^0 peak with fully operational central tracking chambers, silicon microvertex detector and electromagnetic calorimeters. Multihadronic Z^0 decays were selected using the criteria described in [3]. Charged tracks were required to have at least 20 hits in the jet chamber, to have a measured momentum in the $r\phi$ plane of at least 0.150 GeV/c and to pass within 5 cm of the nominal beam interaction point in the $r\phi$ plane. No requirement on hits in the silicon microvertex detector was made at this stage. At least seven such charged tracks were required per event, which suppressed the residual contamination from $e^+e^- \to \tau^+\tau^-$ to less than 0.1%[4].

In each event, charged tracks and those electromagnetic clusters not associated to charged tracks, were grouped into jets using the scaled invariant mass algorithm described in [5] with the E0 recombination scheme and the invariant mass-squared cut-off set to 49 $(\mathrm{GeV}/c^2)^2$. This value was chosen so as to include the maximum number of tracks from the jet containing the B hadron whilst minimizing the number of tracks from nearby gluon jets. It was required that the two highest energy jets be in opposite hemispheres, where the hemispheres are defined with respect to the thrust axis calculated using the same tracks and clusters as used in the jet finding. This requirement removed about 3% of the data. A total of 527 998 events satisfied these event selection and detector performance criteria.

Hadronic Z^0 decays were generated with the Jetset 7.3[6] Monte Carlo program tuned to OPAL data as described in [7] using parameters described in [8] and using the Peterson fragmentation function[9] for c and b quarks. These events were passed through a detailed simulation[10] of the OPAL detector and subjected to the same pattern recognition and reconstruction algorithms as the data. During the analysis, the differences between the $r\phi$ parameters[2] d_0 and ϕ_0 of the reconstructed tracks and of their associated generated particles were increased by a factor of 1.2 to account for systematic misalignments in the data that were not included in the Monte Carlo simulation. This Monte Carlo sample is referred to as the full detector simulation. Additional Monte Carlo samples, not subjected to the simulation of the OPAL detector are referred to as generator level.

4 Secondary Vertex Reconstruction

In order to find secondary vertices, a vertex fit was attempted in each of the two highest energy jets separately. Each track used in these vertex fits was required to have a least one hit in the silicon microvertex detector. All such tracks in the jet were fitted to a common vertex

[2]The $r\phi$ parameters describing a track reconstructed in the OPAL detector are κ, the curvature, d_0 the distance of closest approach to the origin in the $r\phi$ plane and ϕ_0, the azimuthal angle of the tangent to the track at the point of closest approach.

point in the $r\phi$ plane and the track with the largest contribution to the χ^2 removed if its value was greater than four. The procedure was repeated until no further tracks were removed, or there were fewer than four remaining tracks. For each successfully reconstructed secondary vertex, the apparent decay length in $r\phi$ with respect to the average primary vertex position was calculated[11] along with its error. The method used to obtain the average primary vertex position is described in [12]. The decay length was signed such that it was positive if the angle between the jet momentum vector and the vector from the primary to the secondary vertex was less than 90°, otherwise it was negative. In order to accept only well measured decay lengths, the error on the decay length was required to be less than 600μm. The average projected decay length is 2.1mm for B hadrons and the typical decay length error 150μm.

A secondary vertex with at least four associated tracks was found in 66% of the highest energy jets, and 58% of the second highest energy jets. Figure 1 shows the decay lengths of these vertices in the data and the Monte Carlo sample as well as the separate contributions in the Monte Carlo from uds[3], c and b quark events. There is a slight discrepancy between data and Monte Carlo at large negative decay lengths and at positive decay lengths. These discrepancies are related to the resolution of the track parameters, and the input values of the b lifetime and fragmentation function and are discussed in Section 10.

Figure 1 shows that above 0.2 cm, the decay length distribution is dominated by b quark events. Figure 2 shows the quark purity, obtained from the Monte Carlo simulation, defined as the fraction of vertices coming from b, c and uds events, as a function of decay length. The method is not efficient at reconstructing vertices from $Z^0 \to c\overline{c}$ events because of the requirement that there be at least four charged tracks per secondary vertex, and hence the charm fraction changes much less than the bottom fraction.

Using the decay length of these reconstructed secondary vertices, samples of events with b purities varying from about 13% to 89% were selected and used in the subsequent analysis.

5 Charged Particle Multiplicity

If the vertex fit was successful in either of the two highest energy jets, the charged particle multiplicity in the hemisphere opposite that containing the jet was calculated. The hemispheres were defined by the thrust axis as described above. The multiplicity measurement was made in the opposite hemisphere to avoid the bias that would otherwise be caused by the minimum four track requirement. In calculating the charged particle multiplicity, the standard track criteria described previously were used without any requirement on hits in the silicon microvertex detector. Figure 3 shows the uncorrected charged particle multiplicity in the hemispheres opposite those containing a reconstructed secondary vertex with different values of decay length. The average charged particle multiplicity increases with decay length in the opposite hemisphere and hence with b purity. The Monte Carlo simulation agrees well with the data at all decay lengths.

Using the relationship between decay length and b purity shown in figure 2, the average charged

[3]Throughout this paper we use the notation uds(c) to refer to a mixture of $Z^0 \to u\overline{u}$, $Z^0 \to d\overline{d}$, $Z^0 \to s\overline{s}$ ($Z^0 \to c\overline{c}$) events in their Standard Model ratios.

particle multiplicity was plotted against b purity. If vertices were reconstructed in both hemispheres of an event then the multiplicity opposite each of them was used.

The measured charged particle multiplicity was corrected for detector acceptance and efficiency as well as the introduction of spurious tracks from photon conversions and interactions using an unfolding matrix derived from the full detector simulation as described in [13]. No correction for initial state radiation was made. After this procedure, the multiplicity is defined as the total number of all promptly produced stable charged particles and those produced in the decays of particles with lifetimes shorter than 3×10^{-10} sec. This means that charged decay products from K^0_s, hyperons and weakly decaying b and c flavoured hadrons are included in the definition, regardless of how far away from the interaction point the decay actually occurred.

The unfolding matrix was calculated separately for each bin of decay length in the opposite hemispheres. Applying the corrections increased the mean multiplicity, $\bar{n}$, by between 3% and 5% depending on the decay length. Making no decay length cuts, a hemisphere multiplicity of 10.651 ± 0.005 was obtained, which is to be compared with the published OPAL value of $10.70 \pm 0.02 \pm 0.19$[13].

Using the Monte Carlo simulation, the variation of the multiplicity in the opposite hemisphere with decay length was studied for each flavour separately. To account for the small correlations observed we made corrections of between -0.2% and 0.9%.

The hemisphere multiplicity after correction is plotted against b purity in figure 4. The hemisphere multiplicities in b quark events, $\bar{n}_{\rm b}$, and in non-b quark events, $\bar{n}_{\rm udsc}$, separately, were extracted by fitting the data to the form

$$\bar{n} = (1 - \mathcal{P}_{\rm b})\bar{n}_{\rm udsc} + \mathcal{P}_{\rm b}\bar{n}_{\rm b} \qquad (1)$$

where $\mathcal{P}_{\rm b}$ is the b purity in a particular decay length bin. In order to treat $\bar{n}_{\rm udsc}$ as a single variable in the fit, small corrections of between -0.4% and 0.0% were applied to account for the varying charm contribution. These corrections were obtained from the Monte Carlo which provides a good description of charm decays. The results of the fit were

$$\bar{n}_{\rm b} = 11.71 \pm 0.03 \quad \text{and} \quad \bar{n}_{\rm udsc} = 10.32 \pm 0.01.$$

In order to compare the value of $\bar{n}_{\rm b}$ with that from light quarks only, $\bar{n}_{\rm uds}$, another fit was performed of the form

$$\bar{n} = \mathcal{P}_{\rm uds}\bar{n}_{\rm uds} + \mathcal{P}_{\rm c}\bar{n}_{\rm c} + \mathcal{P}_{\rm b}\bar{n}_{\rm b}$$

where $\bar{n}_{\rm c}$ is the charged particle multiplicity per hemisphere in charm events and $\mathcal{P}_{\rm c}$ and $\mathcal{P}_{\rm uds}$ are the charm and light quark purities respectively. This procedure relied on the fact the charm purity as well as the b-purity varied with decay length. The charm correction was not made prior to this fit. The results were

$$\begin{aligned} \bar{n}_{\rm uds} &= 10.21 \pm 0.07 \\ \bar{n}_{\rm c} &= 10.73 \pm 0.25 \\ \bar{n}_{\rm b} &= 11.72 \pm 0.04 \end{aligned}$$

where secondary tracks from the decays of K^0_s and Λs are included. The large error on $\bar{n}_{\rm c}$ reflects the small variation of $\mathcal{P}_{\rm c}$ with decay length. The result for $\bar{n}_{\rm b}$ hardly changed although the error increased. The three results are highly correlated.

Taking into account these correlations, the difference in charged particle multiplicity between b quark and light quark *events* is

$$\delta_{\rm bl} = 2 \times (\bar{n}_{\rm b} - \bar{n}_{\rm uds}) = 3.02 \pm 0.05.$$

6 Impact Parameter Distributions

The hemisphere charged multiplicity of $Z^0 \to b\overline{b}$ events has two main components; the tracks from the decay of the B hadron, including the subsequent charm decay, and the rest of the fragmentation tracks. The tracks from the B hadron in general have non-zero impact parameters with respect to the primary vertex due to the relatively long lifetime of the b quark, whereas most of the other tracks come from the primary vertex.

In order to determine the number of tracks that originated from the decays of the B hadrons and their daughter charmed hadrons, we used a sub-sample of tracks with the best impact parameter resolution, as described below. The impact parameter distributions of these tracks were used to determine the fraction of tracks, $f^{\rm B}$, originating from B decays and the fraction, $f^{\rm pri}$, originating from the primary vertex. These fractions were then applied to the total numbers of tracks to obtain the number of tracks from B decay and the primary vertex respectively. As the impact parameter resolution is momentum dependent, the tracks were divided into several momentum bins and the fractions calculated for each momentum and decay length bin separately.

In addition to the standard charged track criteria described above, the tracks used in the determination of $f^{\rm B}$ and $f^{\rm pri}$ were required to have 2 silicon microvertex detector hits and $\phi_j > 0.4$ rad where ϕ_j is the angle between the plane formed by the track and the axis of the jet containing it and the plane formed by the jet and the z-axis. Tracks with ϕ_j close to zero carry little lifetime information when projected into the $r\phi$ plane even if they originate from long lived B hadrons.

The impact parameter is defined as the distance of closest approach, in the $r\phi$ plane, of the track to the primary vertex position. The primary vertex was determined on an event by event basis as described in [8], except that the primary vertex fit was repeated for each track separately excluding the track in question from the fit. This prevented the assignment of artificially small impact parameters to tracks that would otherwise dominate the primary vertex calculation. The sign of the impact parameter was positive if the angle in the $r\phi$ plane between the vector from the primary vertex position to the point of closest approach of the track and the axis of the jet containing the track was less than 90°, otherwise the sign was negative.

Figure 5 shows the impact parameter distributions of tracks in the opposite hemispheres, for three different decay lengths, within a particular range of momentum. The distributions become more asymmetric as the b fraction increases indicating the increasing contribution from tracks coming directly from the B hadron or subsequent charmed hadron decays. The solid lines on the figures are results of the fits described below.

The impact parameter distributions shown in figure 5 receive contributions from the following sources:

- Primary tracks: Tracks from primary event vertices.
- Bottom tracks: Tracks from B hadron decay vertices and cascade b$\rightarrow$c charm decay vertices.
- Charm tracks: Tracks from directly produced charm decay vertices.
- Secondary tracks: Tracks from K^0, Λ *etc.* decays, interactions in the detector *etc.*

In the Monte Carlo simulation, the contribution from primary tracks is symmetric about zero whereas the bottom contribution is heavily skewed to positive values. The charm contribution is similar to the primary but slightly skewed to positive values. The contribution from secondary tracks is much broader than the others and comes mainly from interactions in the detector.

The fractions $f^{\rm B}(p, L)$ and $f^{\rm pri}(p, L)$ were extracted separately in 100 bins of momentum (p) and decay length (L) from distributions similar to those shown in figure 5. Each distribution was fitted to the sum of a primary plus a bottom contribution after first subtracting the estimated charm and secondary contributions. The parameterization of each contribution is discussed below and summarized in table 1. The χ^2 fits were performed with two free parameters in each distribution, the fraction of bottom tracks and a resolution scale factor s, described below. The number of impact parameter bins in each distribution was adjusted so that each bin had at least 10 entries.

The contributions from each source were parameterized as follows:

Primary Contribution

The primary contribution was parameterized as a delta function at zero impact parameter convoluted with a resolution function obtained from the data. The resolution function was obtained by taking the negative half of the impact parameter distribution for tracks in hemispheres opposite those containing a reconstructed secondary vertex with decay lengths in the range -0.1 to 0.0 cm, where the b quark contribution is smallest. The function was then symmetrized about zero. The charged particle multiplicity of a hemisphere changes with decay length in the opposite hemisphere and because this might have an effect on track resolution, the width of the resolution function was allowed to scale by a factor s. The resolution function was constructed separately for the 10 momentum bins.

Bottom Contribution

The bottom contribution was parameterized as a physics function convoluted with the same resolution function as described above. The physics function was obtained from the impact parameter distribution of bottom tracks in the generator level Monte Carlo with no detector effects included. The physics function was obtained separately in each momentum bin.

Studies with the full detector simulation suggested that the resolution of bottom tracks appears to be slightly worse that that for primary tracks. This is due to errors in the signing of the

impact parameters due to errors in the reconstruction of the jet axis. A sign error makes no difference to the primary track distribution but will turn a bottom track with large positive impact parameter into one with a large negative value which will worsen the calculated resolution. In order to account for this effect a small number (2.5%) of entries on the positive side of the bottom distribution were randomly switched to the negative side.

The bottom contribution, as given by the fits, was 3% at low momentum and small decay lengths, rising to above 80% at high momentum and large decay lengths.

Charm Contribution

The shape of the charm contribution was parameterized in the same way as for the bottom contribution but with no switching of impact parameter signs. The size of the charm contribution was obtained from the full detector simulation.

The subtracted charm contribution was about 1% at low momentum, was 4% at high momentum and large decay lengths and had a maximum of 15% at high momentum and small decay lengths.

Secondary Contribution

The shape of the secondary contribution was obtained from the full detector simulation. The size of the secondary contribution was obtained by normalizing the Monte Carlo distribution to the data in the region outside the impact parameter range used in the fits. The secondary contribution includes tracks from the decays of K^0_s and hyperons that come from B hadron decay.

The subtracted secondary contribution was about 7% at low momentum falling to about 1% at high momentum.

7 B Hadron Decay Multiplicity

In order to calculate the B hadron decay multiplicity, the fitted fractions of bottom tracks $f^{\mathrm{B}}(p, L)$ were multiplied by the total number of tracks $N_{\mathrm{tot}}(p, L)$, satisfying the standard track cuts, and corrected for reconstruction and analysis losses. The results from the 10 momentum bins were then summed to give the mean number of tracks from B hadron decay

$$\bar{n}^{\mathrm{B}}(L) = \sum_p \frac{f^{\mathrm{B}}(p, L) N_{\mathrm{tot}}(p, L)}{\varepsilon_{\mathrm{rec}}(p)\varepsilon_{\mathrm{cut}}(p) N_{\mathrm{hem}}(L)}$$

where $N_{\mathrm{hem}}(L)$ is the number of hemispheres with a reconstructed vertex in the required decay length range.

The track reconstruction efficiency, $\varepsilon_{\mathrm{rec}}$, was obtained from the full detector simulation

$$\varepsilon_{\mathrm{rec}} = \frac{\text{Number of B hadron decay tracks reconstructed/reconstructed b event}}{\text{Number of B hadron charged decay particles generated/generated b event}}$$

and was calculated separately in each momentum bin. The efficiency varied from about 84% below 0.5 GeV/c to 92% above 2 GeV/c.

The efficiency, $\varepsilon_{\rm cut}$, for tracks to pass the ϕ_j cut and the 2 silicon hit requirement was calculated for each momentum bin as

$$\varepsilon_{\rm cut} = (\varepsilon_{\rm All})_{\rm Data} \times \left(\frac{\varepsilon_{\rm B\ tracks}}{\varepsilon_{\rm All}}\right)_{\rm MC}$$

where each of the terms on the right hand side is calculated according to

$$\varepsilon = \frac{\text{Number of tracks passing cuts}}{\text{Number of tracks reconstructed}}$$

and 'all' refers to all tracks and 'B tracks' to those from B hadron decay. The first term is calculated solely from the data whereas the second, small correction, comes from the full detector simulation. The efficiency $\varepsilon_{\rm cut}$ was approximately 45%, falling slightly with momentum.

The average number of primary tracks, $\bar{n}^{\rm pri}$, was found in a similar way using $f^{\rm pri}$ instead of $f^{\rm B}$. The second term in $\varepsilon_{\rm cut}$ and $\varepsilon_{\rm rec}$ were calculated using primary tracks instead of B tracks.

The numbers of bottom tracks and primary tracks per hemisphere are plotted against b purity in figure 6. The b purity corresponding to a given decay length bin was obtained from the Monte Carlo simulation as described above. The non-statistical scatter of the data is due to systematic uncertainties in the determination of the purity which is discussed in Section 10.

The data shown in figure 6 were fitted with straight lines of the form

$$\bar{n}^{\rm B} = (1-\mathcal{P}_{\rm b})\,\bar{n}^{\rm B}_{\rm udsc} + \mathcal{P}_{\rm b}\bar{n}^{\rm B}_{\rm b} \quad \text{and} \quad \bar{n}^{\rm pri} = (1-\mathcal{P}_{\rm b})\,\bar{n}^{\rm pri}_{\rm udsc} + \mathcal{P}_{\rm b}\bar{n}^{\rm pri}_{\rm b}$$

where $\bar{n}^{\rm B}_{\rm udsc}$, $\bar{n}^{\rm B}_{\rm b}$, $\bar{n}^{\rm pri}_{\rm udsc}$ and $\bar{n}^{\rm pri}_{\rm b}$ are the number of B tracks in udsc events, the number of B tracks in b events, the number of primary tracks in udsc events and the number of primary tracks in b events. The production of $\rm b\overline{b}$ pairs during fragmentation and hence $\bar{n}^{\rm B}_{\rm udsc}$ was expected to be very small.

The results were

$$\begin{aligned}
\bar{n}^{\rm B}_{\rm udsc} &= 0.026 \pm 0.013 \\
\bar{n}^{\rm B}_{\rm b} &= 5.025 \pm 0.042 \\
\bar{n}^{\rm pri}_{\rm udsc} &= 8.707 \pm 0.014 \\
\bar{n}^{\rm pri}_{\rm b} &= 5.515 \pm 0.042
\end{aligned}$$

where contributions from secondary decays of $\rm K^0$s and Λs are not included. Constraining $\bar{n}^{\rm B}_{\rm udsc}$ to be zero yielded $\bar{n}^{\rm B}_{\rm b} = 5.059 \pm 0.024$.

Instead of summing over momentum bins, $\bar{n}^{\rm B}$ and $\bar{n}^{\rm pri}$ were plotted against b purity in each momentum bin separately. From these $\mathrm{d}\bar{n}^{\rm B}_{\rm b}(p)$ and $\mathrm{d}\bar{n}^{\rm pri}_{\rm b}(p)$ were derived as shown in table 2. Figure 7 shows $\mathrm{d}\bar{n}^{\rm B}_{\rm b}/\mathrm{d}p$ and $\mathrm{d}\bar{n}^{\rm pri}_{\rm b}/\mathrm{d}p$. The tracks from B hadron decay have a much harder momentum spectrum than the primary tracks in b events, reflecting the hard fragmentation function of b quarks. The mean momentum of the B and primary tracks in b events and primary tracks in non-b events was found to be

$$\begin{aligned}
\langle p\rangle^{\rm B}_{\rm b} &= 3.78 \pm 0.05\ \text{GeV}/c \\
\langle p\rangle^{\rm pri}_{\rm b} &= 1.33 \pm 0.04\ \text{GeV}/c \\
\langle p\rangle^{\rm pri}_{\rm udsc} &= 2.71 \pm 0.01\ \text{GeV}/c
\end{aligned}$$

These measurements were used to measure the mean scaled energy $\langle x_E \rangle_{\rm b}$ carried by b flavoured hadrons as described in section 9.

8 Contribution from $\rm K^0_S$ and Λ Decays

In order to compare the measurement of the mean B decay multiplicity with previous publications, it was necessary to include the contribution from $\rm K^0_S$, Λ and other hyperons. The measurements of $\bar{n}_{\rm b}^{\rm B}$, $\bar{n}_{\rm b}^{\rm pri}$ and $\bar{n}_{\rm udsc}^{\rm pri}$, which do not include contributions from decays of $\rm K^0_S$ and Λ, were combined with the measurements of $\bar{n}_{\rm b}$ and $\bar{n}_{\rm udsc}$ which do include contributions from these decays.

Ignoring contributions from direct charm production in b events, which are expected to be very small,

$$\bar{n}_{\rm b} = \bar{n}_{\rm b}^{\rm pri} + \bar{n}_{\rm b}^{\rm K\Lambda} + \bar{n}_{\rm b}^{\rm B} + \bar{n}_{\rm b}^{\rm B\to K\Lambda}$$
$$\bar{n}_{\rm udsc} = \bar{n}_{\rm udsc}^{\rm pri} + \bar{n}_{\rm udsc}^{\rm K\Lambda} + \bar{n}_{\rm udsc}^{\rm charm}$$

where $\bar{n}_{\rm udsc}^{\rm K\Lambda}$ is the number of tracks from $\rm K^0_S$ and Λ in udsc hemispheres and $\bar{n}_{\rm udsc}^{\rm charm}$ is the number of charm decay tracks per udsc hemisphere. The number of tracks from $\rm K^0_S$ and Λ in b events has two components; the number originating from B hadron decay, $\bar{n}_{\rm b}^{\rm B\to K\Lambda}$, and the rest, $\bar{n}_{\rm b}^{\rm K\Lambda}$.

The mean B decay multiplicity including contributions from $\rm K^0_S$ and Λ is hence

$$\bar{n}_{\rm b}^{\rm B} + \bar{n}_{\rm b}^{\rm B\to K\Lambda} = \bar{n}_{\rm b} - \bar{n}_{\rm b}^{\rm pri} - \bar{n}_{\rm b}^{\rm K\Lambda}$$

The value of $\bar{n}_{\rm b}^{\rm K\Lambda}$ was estimated from the data by assuming that the ratio of tracks from $\rm K^0_S$ and Λ decays to primary tracks is the same in the non-leading (not from B decay) part of b events as it is in udsc events *i.e.*

$$\bar{n}_{\rm b}^{\rm K\Lambda} = \frac{\bar{n}_{\rm udsc}^{\rm K\Lambda}}{\bar{n}_{\rm udsc}^{\rm pri}} \times \bar{n}_{\rm b}^{\rm pri}$$

where

$$\bar{n}_{\rm udsc}^{\rm K\Lambda} = \bar{n}_{\rm udsc} - \bar{n}_{\rm udsc}^{\rm pri} - \bar{n}_{\rm udsc}^{\rm charm}$$

The value $\bar{n}_{\rm udsc}^{\rm charm}$ was taken to be 0.52 ± 0.13. This was calculated by assuming the ratio of $\rm D^*$:D production was 3:1 and using the $\rm D^*$ branching ratios from [14] combined with D decay multiplicities from [15] to give 2.39 ± 0.14 tracks per stable D decay[4] where the error includes the effect of varying the $\rm D^*$ rate from 0 to 100%. This was converted to the number of charm tracks per udsc event using the Standard Model values of $\Gamma_{\rm c\bar{c}}/\Gamma_{\rm had} = 0.171$ and $\Gamma_{\rm b\bar{b}}/\Gamma_{\rm had} = 0.217$. Jetset predicts $\bar{n}_{\rm udsc}^{\rm charm} = 0.522$ and Eurodec[16] 0.471.

Hence

$$\bar{n}_{\rm b}^{\rm B} + \bar{n}_{\rm b}^{\rm B\to K\Lambda} = 5.51 \pm 0.05$$

[4]Transition pions from $\rm D^{**}$ or $\rm D^*$ decays were considered to be primary and not included in $\bar{n}_{\rm udsc}^{\rm charm}$. Corrections due to $\rm D_s$ and charm baryon decays are ~ 0.01 tracks in Jetset and ~ 0.04 tracks in Eurodec and have not been included.

9 The b quark Fragmentation Function

The measurements of $\bar{n}_{\rm b}^{\rm B}$ and $\bar{n}_{\rm b}^{\rm pri}$ were used to estimate the mean scaled energy, $\langle x_E \rangle_{\rm b}$ carried by b flavoured hadrons in Z^0 decays, where $x_E = 2E_{\rm hadron}/W$, $E_{\rm hadron}$ is the energy of the B hadron and W is the nominal centre-of-mass energy. As $\langle x_E \rangle_{\rm b}$ increases and the B hadron takes more of the available energy, the energy remaining to create primary particles decreases and $\bar{n}_{\rm b}^{\rm pri}$ decreases. The number of tracks from the B hadron, $\bar{n}_{\rm b}^{\rm B}$, is fixed but as the B hadron takes more energy, the momentum distribution of these tracks will harden and $\langle p \rangle_{\rm b}^{\rm B}$ will increase. A number of methods of estimating $\langle x_E \rangle_{\rm b}$ were investigated. Two complimentary methods, the mean momentum of B hadron decay tracks, $\langle p \rangle_{\rm b}^{\rm B}$, and the number of primary tracks in b events, $\bar{n}_{\rm b}^{\rm pri}$ were chosen.

The relationships between $\langle p \rangle_{\rm b}^{\rm B}$ and $\langle x_E \rangle_{\rm b}$ and $\bar{n}_{\rm b}^{\rm pri}$ and $\langle x_E \rangle_{\rm b}$ were obtained from generator level Jetset 7.3 Monte Carlo events with standard OPAL parameters and Peterson fragmentation with $\epsilon_{\rm b}$ between 0.001 an 0.01. There is a linear relationship between $\langle p \rangle_{\rm b}^{\rm B}$ and $\langle x_E \rangle_{\rm b}$ that is independent of the fragmentation model. The relationship between $\bar{n}_{\rm b}^{\rm pri}$ and $\langle x_E \rangle_{\rm b}$ is nearly linear over the range of $\langle x_E \rangle_{\rm b}$ considered but may depend on the shape of the fragmentation function.

The following results were obtained using $\langle p \rangle_{\rm b}^{\rm B}$ and $\bar{n}_{\rm b}^{\rm pri}$ respectively:

$$\langle x_E \rangle_{\rm b} = 0.702 \pm 0.009$$

$$\langle x_E \rangle_{\rm b} = 0.684 \pm 0.004$$

Since the systematic errors on the two methods were found to be similar and dominate the statistical errors, the average of the two results was taken to obtain

$$\langle x_E \rangle_{\rm b} = 0.693 \pm 0.003.$$

This corresponds to $\epsilon_{\rm b} \sim 0.0055$ within the Jetset Model.

10 Systematic Uncertainties

There are two classes of systematic uncertainty in this analysis, those that affected the measured multiplicity in each decay length bin and those that affected the assumed purity within that bin. Some sources contributed to both classes. The systematic uncertainties are summarized in table 3.

The main sources of systematic uncertainty are those which determine the shape of the decay length distribution, used to extract the b-purity. The discrepancy on the positive side of the distribution (figure 1) can be removed by increasing the b lifetime in the Monte Carlo to 1.7ps, making the b fragmentation harder or increasing the scaling of the track parameters in the Monte Carlo as described in section 3. The systematic uncertainties in the results due to these effects were estimated as follows:

- The average b lifetime was varied by ± 0.10ps about its central value of 1.55ps [17].

- The parameters ϵ_b and ϵ_c, that control the b and c quark fragmentation, were varied from 0.0095 to 0.0025 and 0.057 to 0.046 respectively. These are equivalent to the averages of $\langle x_E \rangle_b$ and $\langle x_E \rangle_c$ given in [4, 18, 19].
- The Monte Carlo scaling described in section 3 was varied between 1.0 (no scaling) and 1.4.

As a cross check every reconstructed decay length in the Monte Carlo was increased by a factor of 15% which also removed the discrepancy between data and Monte Carlo and changed the results by less than the systematic uncertainties attributed to the sources given above.

Other factors that influence the shape of the decay length distribution are the production rates of b and c quarks, and because of the four track requirement, the mixture of B hadrons produced and the decay multiplicities of the B hadrons.

- The ratios $\Gamma_{b\bar{b}}/\Gamma_{had}$ and $\Gamma_{c\bar{c}}/\Gamma_{had}$ were varied from 0.204 to 0.232 and 0.133 to 0.209 respectively, corresponding approximately to the errors given in[19, 20].
- The fractions of B_s and Λ_b produced were changed from half to double their nominal values of 12% and 9% respectively, and the ratio of B_u to B_d was changed by $\pm 20\%$.
- The B hadron decay multiplicity (including K_s^0 and Λ decays) was varied by ± 0.5 tracks.

The following procedures were specific to the estimation of the systematic uncertainties on $\bar{n}_b$, $\bar{n}_{udsc}$ and δ_{bl}:

- The correlation and charm corrections are model dependent. The fits were repeated without these corrections and the difference in the results treated as a source of systematic uncertainty.
- Since the same correction procedure as described in [13] has been used with essentially the same Monte Carlo program, it was assumed that this analysis is subject to the same acceptance and efficiency systematic uncertainties as described in [13]. The contributions to the uncertainty in single hemisphere multiplicity are 0.2% from detector simulation, 1.5% from track and event selection and 0.9% from model dependence giving an overall systematic uncertainty of 1.8%. This correction should be treated as an overall scale uncertainty and applied to both $\bar{n}_{uds}$ and $\bar{n}_b$, but not to the ratio.
- To account for any decay length dependence in this procedure, the analysis was repeated with the corrections derived from three decay length bins only and by applying the same global correction to all 10 decay length bins.

Although the fitting of the impact parameter distributions relies mainly on the data itself to provide the resolution function, the secondary contribution and especially the charm contribution rely on Monte Carlo simulation and are possible sources of systematic error.

- The charm contribution in the impact parameter fits was varied by 25% to account for uncertainties in $\Gamma_{c\bar{c}}/\Gamma_{had}$ and the charm decay multiplicity.

- The secondary contribution in the impact parameter fits was taken directly from the full detector simulation instead of being normalized to the data.
- The B physics function used in the fits is the sum of the contributions of tracks coming directly from B decays and of those coming from cascade B$\rightarrow$D decays. The latter has on average larger impact parameters. The relative amounts of these two contributions came from the Monte Carlo simulation and a variation of $\pm 20\%$ in the fraction coming directly from B decays was treated as a possible source of systematic uncertainty. This variation is equivalent to changing the total B decay multiplicity by ± 1 track whilst keeping the amount of cascade constant, or alternatively in terms of the lifetime content of the tracks, changing the $\mathrm{D}^{\pm}$ fraction from zero to twice its nominal value.
- The number of B tracks whose impact parameter signs were changed was varied from 0% to 5%.
- The efficiency for tracks to pass the additional track cuts, $\varepsilon_{\mathrm{cut}}$, was mainly determined from the data. However, the efficiency for reconstructing a track in the OPAL detector, $\varepsilon_{\mathrm{rec}}$, was obtained from the full detector simulation and could be a source of systematic error, especially if there were flavour dependent effects that depended on the environment surrounding a track. The efficiency was calculated separately for each type of track (B tracks, D decay tracks, primary tracks in uds events, primary tracks in b events *etc.*) and for events with less and more than 20 tracks generated and the largest variations used to estimate the systematic uncertainty.
- The resolution scaling factor, s, was a free parameter in the fits since the impact parameter resolution in the Monte Carlo simulation was seen to depend on the decay length in the opposite hemisphere. The scaling factor was changed by $\pm 20\%$ around the value determined by the fit for B tracks only.

The extraction of $\langle x_E \rangle_{\mathrm{b}}$ from $\langle p \rangle_{\mathrm{b}}^{\mathrm{B}}$ and $\bar{n}_{\mathrm{b}}^{\mathrm{pri}}$ relies on the modelling of B hadron decay and light quark fragmentation. The model dependence was estimated as follows:

- The procedure was repeated using Eurodec instead of Jetset to model B hadron decays.
- The light quark fragmentation parameters in Jetset were varied by the one standard deviation errors given in [7]. The QCD scale parameter Λ_{QCD} was varied between 0.30 and 0.33 GeV. The parton shower cut-off parameter Q_0 was varied between 0.7 and 1.8 GeV. The parameter σ_q that controls the transverse momentum was varied between 0.31 and 0.39 GeV and the parameter a that controls the fragmentation function was varied between 0.06 and 0.23.

Several additional cross checks were performed. In all cases, the variations in the results were within the systematic uncertainties from the sources already described and were not considered as additional sources of uncertainty.

- The number of tracks required to form a vertex was changed by ± 1 from the standard value of four. This change had a significant effect on the b purity in each decay length bin and a dramatic effect on the vertex finding efficiency, but the effect on the overall result was small.

- The requirement that there be two silicon hits per track was loosened to one per track. This increased the number of tracks used in the analysis but introduced more poorly measured tracks and secondary tracks. There was a significant change in the result but it was less than the systematic error assigned to the secondary track contribution for instance.
- The ϕ_j cut was changed from 0.4 by ± 0.2 rad. This changed the amount of lifetime information contained in the impact parameter distributions. The changes to the results were small.
- The impact parameters were calculated with respect to the event by event primary vertex position. The analysis was repeated using the average primary vertex position which worsened the impact parameter resolution and might have introduced a different correlation between the two hemispheres. The effect on the results was small.
- The analysis was repeated with 1991 data which had two missing silicon detector ladders. The changes to the results were well within the systematic errors quoted for detector resolution.

11 Comparison of Multiplicity with QCD Predictions

QCD calculations using the Modified Leading Log Approximation (MLLA)[21] combined with Local Parton-Hadron Duality (LPHD)[22] are expected to describe the gross features of hadronic systems, such as multiplicity distributions, without invoking phenomenological fragmentation schemes. This approach is expected[23] to be particularly successful in the case of e^+e^- annihilation into heavy quarks of mass M_Q at centre of mass energies W where $W \gg M_Q \gg \Lambda_{QCD}$. In particular, there is a prediction[24] that the difference in multiplicity between heavy quark and light quark events is independent of centre of mass energy.

Due to the suppression of forward gluons in the angular region around the heavy quark direction, MLLA predicts that the companion or non-leading multiplicity $\Delta N(Q\overline{Q};W)$ of light hadrons accompanying the heavy quark Q, excluding the decay products of the on-shell heavy hadron is less than the multiplicity in a light quark event at the same centre of mass energy, $N(q\overline{q};W)$

$$\Delta N(Q\overline{Q};W) = N(q\overline{q};W) - N(q\overline{q};\sqrt{e}\cdot M_Q) + \mathcal{O}(\alpha_s(M_Q^2)N(q\overline{q};M_Q))$$

where e is the base of natural logarithms.

Hence ignoring higher order terms, MLLA predicts that $N(q\overline{q};W) - \Delta N(Q\overline{Q};W)$ is independent of centre of mass energy. The difference in multiplicity between heavy and light quark events at the same centre of mass energy can be written as

$$\begin{aligned} \delta_{Ql} &= \Delta N(Q\overline{Q};W) + N_Q^{decay} - N(q\overline{q};W) \\ &= N_Q^{decay} - N(q\overline{q};\sqrt{e}\cdot M_Q) \end{aligned}$$

where N_Q^{decay} is the multiplicity from the decay of heavy hadrons containing the heavy quark Q. Thus MLLA predicts that δ_{Ql} is independent of centre of mass energy.

An estimate of the numerical value of $\delta_{\rm bl}$ is given in [24] using $\sqrt{e}\cdot M_{\rm B} = \sqrt{e}\cdot 4.8 = 7.9$ and low energy data corrected for charm contributions, which yields $N(\mathrm{q\overline{q}};\sqrt{e}\cdot M_{\rm B}) = 5.5 \pm 0.7$. Assuming $N_{\rm b}^{\rm decay} = 11.0 \pm 0.2$ they get the MLLA prediction that

$$\delta_{\rm bl} = 5.5 \pm 0.8.$$

Additional uncertainties arise from higher order contributions. For example the magnitude of the $\mathcal{O}(\alpha_{\rm s}(M_{\rm Q}^2)N(\mathrm{q\overline{q}};M_{\rm Q}))$ term is expected to be about $0.2 \times 5.5 \sim 1.1$ tracks.

A more naïve approach[25] is to assume that the non-leading multiplicity in heavy quark events is the same as the multiplicity in light quark events at the centre of mass corresponding to the energy left behind after the heavy quarks have fragmented i.e.

$$\Delta N(\mathrm{Q\overline{Q}};W) = N(\mathrm{q\overline{q}};(1-\langle x_E\rangle_{\rm Q})\cdot W)$$

where $\langle x_E\rangle_{\rm Q} = 2E_{\rm Q}/W$ is the mean fraction of the beam energy carried by the heavy hadrons containing the heavy quark Q. Hence

$$\delta_{\rm Ql} = N_{\rm Q}^{\rm decay} + N(\mathrm{q\overline{q}};(1-\langle x_E\rangle_{\rm Q})\cdot W) - N(\mathrm{q\overline{q}};W)$$

Using a parameterization of world average charged particle multiplicity data, corrected to remove the effects of heavy quark production[26],

$$N(\mathrm{q\overline{q}},W) = 2.554 + 0.1252 \times \exp(2.317\sqrt{\ln W})$$

and assuming $\langle x_E\rangle_{\rm b} = 0.7$, $\delta_{\rm bl}$ falls from 6.9 at $W = 20$ GeV to 1.9 at $W = 100$ GeV, with a value of 2.3 at $W = 91.2$ GeV. There is an uncertainty of about ± 0.5 in this prediction due to the charm subtraction.

The Jetset Monte Carlo program also predicts that $\delta_{\rm bl}$ is independent of energy and gives $\delta_{\rm bl} = 2.37$ at $W = 91.2$ GeV.

Figure 8 shows our measurement of $\delta_{\rm bl}$ at 91.2 GeV along with previous measurements[25, 27] at other energies. Also shown are the MLLA and the naïve predictions discussed above. Fitting a straight line of the form $\delta_{\rm bl} = a + bW$ through all the data[5], gave $a = 5.0 \pm 1.3$ and $b = -0.023 \pm 0.019$ which is compatible with the hypothesis that $\delta_{\rm bl}$ is independent of energy. However, we cannot distinguish between the naïve and MLLA predictions with the current results.

12 Conclusions

We have reconstructed secondary vertices in jets. By cutting on the distance of these vertices from the average beam position, samples of events with b purity varying from about 13% to 89% were selected.

[5] Note that some of the errors are correlated between experiments due to a common charm uncertainty. The errors between this measurement and the ones at 29 GeV are largely uncorrelated.

We have measured the charged particle multiplicity in the hemispheres opposite these jets and derived values for the hemisphere charged particle multiplicity in $Z^0 \to b\overline{b}$ events compared to that in non-$b\overline{b}$ events of

$$\bar{n}_{\rm b} = 11.71 \pm 0.03 \pm 0.18 \pm 0.21$$

$$\bar{n}_{\rm udsc} = 10.32 \pm 0.01 \pm 0.07 \pm 0.19$$

where the first error is statistical, the second systematic and the third a common uncertainty due to the acceptance and efficiency correction as described in [13]. The systematic uncertainties are summarized in table 3. The results include contributions from K^0_s and Λ decays.

We find the difference in total charged particle multiplicity between b quark events and light (uds) quark events to be

$$\delta_{\rm bl} = 3.02 \pm 0.05 \pm 0.79.$$

This result is consistent with the naïve model that the non-leading multiplicity in b quark events is the same as that in light quark events at centre of mass energies corresponding to that remaining after the b quarks have fragmented to B hadrons. When combined with data at other energies the result is also consistent with the MLLA prediction that $\delta_{\rm bl}$ should be independent of centre of mass energy.

We have also studied the impact parameter distributions of charged particles in the hemispheres of the events opposite these jets and measured the charged particle decay multiplicity of B hadrons to be

$$\bar{n}^{\rm B} = 5.03 \pm 0.04 \pm 0.49 \quad \text{(Excluding } K^0 \text{ and } \Lambda \text{ decay products)},$$

$$\bar{n}^{\rm B} = 5.51 \pm 0.05 \pm 0.51 \quad \text{(Including } K^0 \text{ and } \Lambda \text{ decay products)}.$$

The latter result can be compared with the predictions of Jetset and Eurodec, including K^0_s and Λ, of 5.211 and 5.135 respectively. It agrees well with lower energy results from CLEO and ARGUS of 5.44 ± 0.10 which is the combined result from charged particle multiplicity measurements of $10.81 \pm 0.05 \pm 0.23$[28] and $10.99 \pm 0.06 \pm 0.29$[29] at the $\Upsilon(4s)$. At the $\Upsilon(4s)$ only B_u and B_d are produced whereas at LEP B_s and B baryons are also produced.

The hemisphere non-leading or primary multiplicity (excluding K^0_s and Λ decays) in b and non-b events were found to be

$$\bar{n}^{\rm pri}_{\rm b} = 5.52 \pm 0.04 \pm 0.34$$

$$\bar{n}^{\rm pri}_{\rm udsc} = 8.71 \pm 0.01 \pm 0.21.$$

From the mean momentum of the B decay products and the number of primary charged particles per b event, the average x_E of b flavoured hadrons was measured to be

$$\langle x_E \rangle_{\rm b} = 0.693 \pm 0.003 \pm 0.030.$$

The result is in excellent agreement with the value obtained independently from high transverse momentum leptons, $\langle x_E \rangle_{\rm b} = 0.697 \pm 0.006 \pm 0.010$[30].

Acknowledgements

Useful comments from V.A.Khoze are gratefully acknowledged. It is a pleasure to thank the SL Division for the efficient operation of the LEP accelerator and their continuing close cooperation with our experimental group. In addition to the support staff at our own institutions we are pleased to acknowledge the
Department of Energy, USA,
National Science Foundation, USA,
Texas National Research Laboratory Commission, USA,
Science and Engineering Research Council, UK,
Natural Sciences and Engineering Research Council, Canada,
Fussefeld Foundation,
Israeli Ministry of Energy and Ministry of Science,
Minerva Gesellschaft,
Japanese Ministry of Education, Science and Culture (the Monbusho) and a grant under the Monbusho International Science Research Program,
German Israeli Bi-national Science Foundation (GIF),
Direction des Sciences de la Matière du Commissariat à l'Energie Atomique, France,
Bundesministerium für Forschung und Technologie, Germany,
National Research Council of Canada,
A.P. Sloan Foundation and Junta Nacional de Investigação Científica e Tecnológica, Portugal.

References

[1] OPAL Collaboration, K.Ahmet *et al.*, Nucl. Instr. and Meth. **A305** (1991) 275.

[2] P.P.Allport *et al.*, Nucl. Instr. and Meth. **A324** (1993) 34.

[3] OPAL Collaboration, G.Alexander *et al.*, Z. Phys. C **52** (1991) 175.

[4] OPAL Collaboration, M.Z.Akrawy *et al.*, Phys. Lett. **263B** (1991) 311.

[5] OPAL Collaboration, M.Z.Akrawy *et al.*, Phys. Lett. **235B** (1990) 389.

[6] T.Sjöstrand, Comp. Phys. Comm **39** (1986) 347;
T.Sjöstrand, M.Bengtsson, Comp. Phys. Comm **43** (1987) 367.

[7] OPAL Collaboration, M.Z.Akrawy *et al.*, Z. Phys. C **47** (1990) 505.

[8] OPAL Collaboration, P.D.Acton *et al.*, Z. Phys. C **58** (1993) 387.

[9] C.Peterson, D.Schlatter, I.Schmitt and P.M.Zerwas, Phys. Rev. D **27** (1983) 105.

[10] J.Allison *et al.*, Nucl. Instr. and Meth. **A317** (1992) 47.

[11] G.J.Barker, *A measurement of the mean B hadron lifetime using the central drift chambers of the OPAL experiment at LEP*, Ph.D Thesis, University of London, 1993.

[12] OPAL Collaboration, P.D.Acton *et al.*, Phys. Lett. **273B** (1991) 355.

[13] OPAL Collaboration, P.D.Acton *et al.*, Z. Phys. C **53** (1992) 539.

[14] CLEO Collaboration, F.Butler *et al.*, Phys. Rev. Letters **69** (1992) 2041.

[15] R.H.Schindler *et al.*, Phys. Rev. D **24** (1981) 78.

[16] A.Ali, B. van Eijk, I. ten Have Nucl. Phys. **B292** (1987) 1.

[17] ALEPH Collaboration, D.Decamp *et al.*, Phys. Lett. **295B** (1992) 174;
DELPHI Collaboration, P.Abreu *et al.*, Z. Phys. C **53** (1992) 567;
L3 Collaboration, B.Adeva *et al.*, Phys. Lett. **270B** (1991) 111;
OPAL Collaboration, P.D.Acton *et al.*, CERN-PPE/93-92, submitted to Z. Phys. C.

[18] ALEPH Collaboration, D.Decamp *et al.*, Phys. Lett. **244B** (1990) 551;
DELPHI Collaboration, P.Abreu *et al.*, Z. Phys. C **56** (1992) 47;
L3 Collaboration, O.Adriani *et al.*, Phys. Lett. **288B** (1992) 412.

[19] ALEPH Collaboration, D.Decamp *et al.*, Phys. Lett. **266B** (1991) 218;
OPAL Collaboration, G.Alexander *et al.*, Phys. Lett. **262B** (1991) 341.

[20] OPAL Collaboration, P.D.Acton *et al.*, Z. Phys. C **58** (1993) 523.

[21] Yu.L.Dokshitzer, V.A.Khoze, A.H.Mueller and S.I.Troyan, *Basics of Perturbative QCD*, ed. Tran Than Van, Editions Frontieres, Paris, 1991.

[22] D.Amati and G.Veneziano, Phys. Lett. **83B** (1979) 87;
Ya.I.Azimov, Yu.L.Dokshitzer,V.A.Khoze and S.I.Troyan, Z. Phys. C **27** (1985) 65.

[23] V.A.Khoze, *Selected perturbative results on heavy quark physics*, DTP/93-32, 1993.

[24] B.A.Schumm, Y.L.Dokshitzer, V.A.Khoze and D.S.Koetke, Phys. Rev. Letters **69** (1992) 3025.

[25] P.C.Rowson *et al.*, Phys. Rev. Letters **54** (1985) 2580.

[26] D.S.Koetke, *A measurement of the Z^0 hadronic branching ratio to bottom quarks and the charged multiplicity of bottom quark events using precision vertex detectors at $E_{\rm cm}$ = 91 GeV*, Ph.D Thesis SLAC-396.

[27] M.Sakuda *et al.*, Phys. Lett. **152B** (1985) 399;
H.Aihara *et al.*, Phys. Lett. **184B** (1987) 299;
W.Braunschweig *et al.*, Z. Phys. C **42** (1989) 17;
B.A.Schumm *et al.*, Phys. Rev. D **46** (1992) 453.

[28] B.Gittelman and S.Stone, *B Meson decay*, *High Energy Electron Positron Physics*, A.Ali and P.Söding (eds), World Scientific Publishing Co. (1988), 273.

[29] ARGUS Collaboration, H.Albrecht *et al.*, Z. Phys. C **54** (1992) 20.

[30] OPAL Collaboration, R.Akers *et al.*, CERN-PPE/93-106, submitted to Z. Phys. C.

Contribution	Shape	Resolution	Size
Primary	δ function	Data	Fit
Bottom	Generator level MC	Data	Fit
Charm	Generator level MC	Data	Full MC
Secondary	Full MC		Data

Table 1: Summary of the source of each contribution to the fits to the impact parameter distributions.

p (GeV/c)	$\langle p \rangle$	$\mathrm{d}\bar{n}^{\mathrm{B}}_{\mathrm{udsc}}(p)$	$\mathrm{d}\bar{n}^{\mathrm{B}}_{\mathrm{b}}(p)$	$\mathrm{d}\bar{n}^{\mathrm{pri}}_{\mathrm{udsc}}(p)$	$\mathrm{d}\bar{n}^{\mathrm{pri}}_{\mathrm{b}}(p)$
0.00 to 0.50	0.34	0.030 ± 0.008	0.392 ± 0.024	1.887 ± 0.007	1.717 ± 0.022
0.50 to 1.00	0.73	0.007 ± 0.005	0.623 ± 0.017	1.775 ± 0.006	1.503 ± 0.016
1.00 to 1.50	1.23	-0.001 ± 0.004	0.584 ± 0.013	1.085 ± 0.004	0.803 ± 0.013
1.50 to 2.00	1.74	0.003 ± 0.003	0.489 ± 0.011	0.737 ± 0.004	0.467 ± 0.011
2.00 to 2.50	2.24	-0.002 ± 0.003	0.415 ± 0.010	0.540 ± 0.003	0.302 ± 0.010
2.50 to 3.00	2.74	0.003 ± 0.003	0.351 ± 0.008	0.404 ± 0.003	0.190 ± 0.009
3.00 to 4.00	3.46	-0.003 ± 0.003	0.562 ± 0.010	0.584 ± 0.003	0.228 ± 0.011
4.00 to 6.00	4.88	0.001 ± 0.004	0.693 ± 0.011	0.658 ± 0.004	0.194 ± 0.012
6.00 to 10.0	7.65	-0.004 ± 0.003	0.578 ± 0.010	0.583 ± 0.003	0.096 ± 0.012
10.0 to 50.0	15.56	-0.007 ± 0.003	0.333 ± 0.008	0.454 ± 0.003	0.011 ± 0.011

Table 2: The number of B tracks and the number of primary tracks per hemisphere in udsc and b events as a function of momentum, p.

Description	$\bar{n}_{\mathrm{udsc}}$	$\bar{n}_{\mathrm{b}}$	δ_{bl}	$\bar{n}_{\mathrm{b}}^{\mathrm{B}}$	$\bar{n}_{\mathrm{b}}^{\mathrm{pri}}$	$\bar{n}_{\mathrm{udsc}}^{\mathrm{pri}}$	$\langle x_E \rangle_{\mathrm{b}}$
b lifetime	0.006	0.001	0.011	0.141	0.108	0.022	0.0036
b fragmentation	0.004	0.010	0.055	0.209	0.045	0.110	0.0030
c fragmentation	0.005	0.016	0.026	0.014	0.039	0.081	0.0021
Resolution scaling	0.017	0.127	0.496	0.307	0.121	0.096	0.0039
$\Gamma_{\mathrm{b\bar{b}}}/\Gamma_{\mathrm{had}}$	0.040	0.031	0.023	0.092	0.076	0.043	0.0041
$\Gamma_{\mathrm{c\bar{c}}}/\Gamma_{\mathrm{had}}$	0.010	0.047	0.135				
B species	0.003	0.040	0.061	0.015	0.010	0.008	0.0017
B decay multiplicity	0.000	0.061	0.178	0.101	0.076	0.006	0.0036
Correlation correction	0.034	0.053	0.064				
Charm correction	0.008	0.056					
Global & 3 bin correction	0.044	0.050	0.561				
Charm contribution				0.118	0.175	0.084	0.0100
Secondary contribution				0.003	0.014	0.005	0.0008
Direct B contribution				0.123	0.108	0.004	0.0158
Sign flipping				0.172	0.176	0.005	0.0139
Efficiency				0.045	0.043	0.074	0.0014
B Resolution scaling				0.037	0.037	0.015	0.0127
Eurodec B decays							0.0023
Light quark fragmentation							0.0090
Total systematic error	0.072	0.183	0.789	0.489	0.344	0.208	0.0294
Acceptance & Efficiency	0.186	0.211	0.054				

Table 3: Summary of systematic error contributions. The contribution due to the acceptance and efficiency correction is an overall scale factor that should be applied to $\bar{n}_{\mathrm{udsc}}$ and $\bar{n}_{\mathrm{b}}$ separately, but not to the ratio.

Figure Captions

Figure 1. The decay length of either of the highest energy jets in the data (points with error bars) and the Monte Carlo (histogram). The contribution to the Monte Carlo from bottom quark events is shown as the shaded histogram, and that from charm quarks and light quarks as the dashed and dotted histograms respectively.

Figure 2. The quark purity as a function of decay length for bottom, charm and light (uds) quarks.

Figure 3. The uncorrected charged particle multiplicity for data (points with error bars) and Monte Carlo (histogram) in the hemispheres opposite reconstructed vertices with decay lengths of (a) -0.1 to 0.0 cm, (b) 0.05 to 0.2 cm, (c) 0.3 to 1.0 cm. These correspond to b purities of about 12%, 48% and 90% respectively. The B decay multiplicity (including K^0_s and Λ decays) in the Monte Carlo was increased to agree with the value measured in this paper.

Figure 4. The charged particle multiplicity in the hemispheres opposite those containing a reconstructed secondary vertex as a function of the b purity of the events. The solid line is a straight line fit through the data points. The errors shown are statistical only and do not include systematic uncertainties in the determination of the b purity.

Figure 5. Distributions of the impact parameters of tracks with momenta in the range 2.0 to 2.5 GeV/c in hemispheres opposite those containing a reconstructed secondary vertex with decay lengths in the range (a) -0.1 to 0.0 cm, (b) 0.05 to 0.2 cm and (c) 0.3 to 1.0 cm. These correspond to samples with b purities of $\sim$12%, $\sim$48% and $\sim$90% respectively. The points with error bars are the data and the solid histograms are the results of the fits described in the text. The almost perfect agreement on the negative side of (a) is due to the fact that this distribution provides the resolution function used by the others.

Figure 6. The charged particle multiplicity, (a) for tracks from B hadron decays and (b) for primary tracks, in the hemispheres opposite those containing a reconstructed secondary vertex, as a function of the b purity of the event. The solid lines are straight line fits through the points. The error bars, which are smaller than the points, are statistical only and do not include systematic uncertainties in the determination of the b purity.

Figure 7. The momentum distributions of charged tracks from B decays (solid points) and primary tracks (open points) in $Z^0 \to b\overline{b}$ events. The error bars are statistical only.

Figure 8. The difference in charged particle multiplicity δ_{bl} between b quark and light quark events as a function of centre of mass energy. The first point is the average of measurements at 29 GeV with common systematics taken into account[24]. The MLLA prediction[24] that δ_{bl} is independent of energy (see text for details) is shown as the solid line. The dotted line indicates the error on this prediction but does not include higher order corrections. The dashed line is the naïve prediciton.

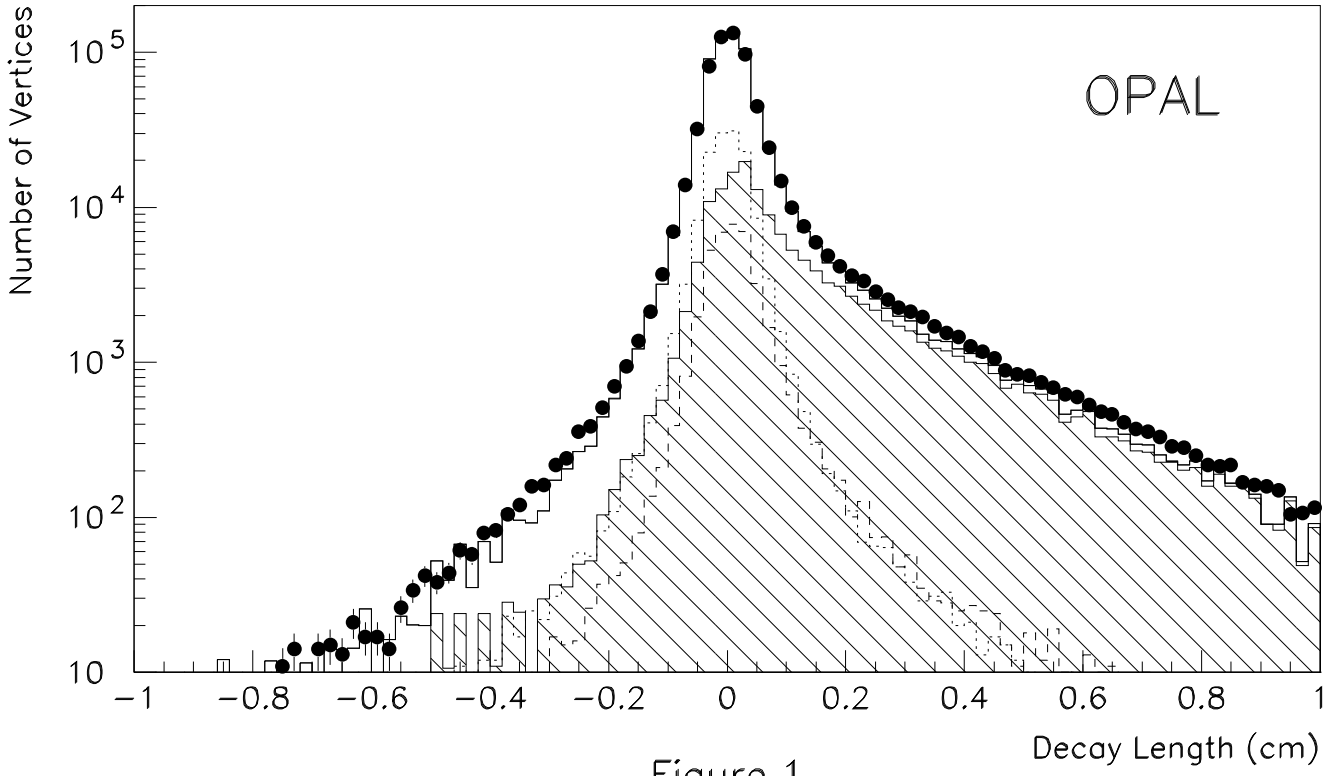

Figure 1

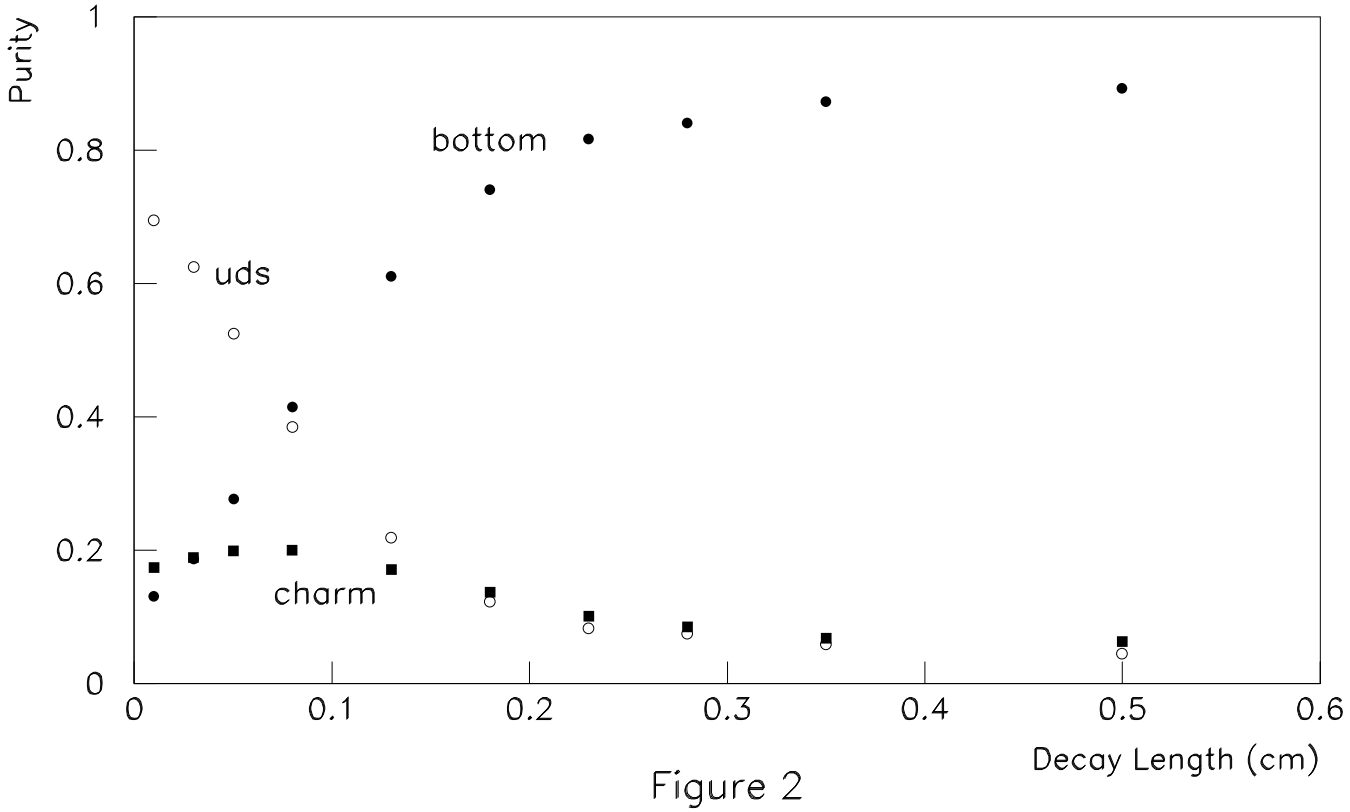

Figure 2

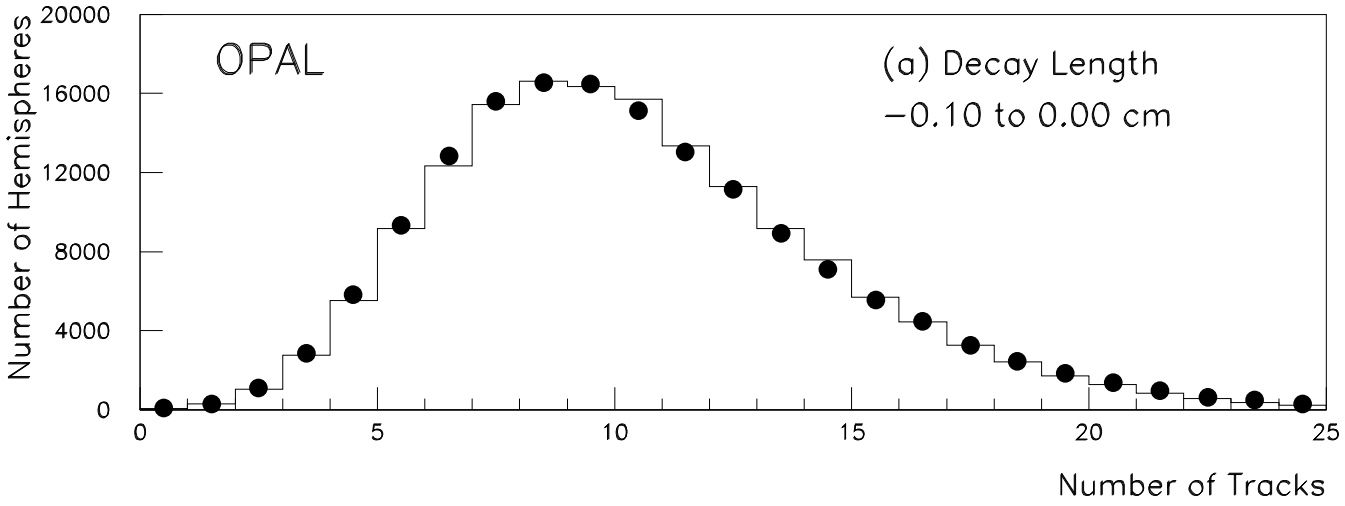
OPAL
(a) Decay Length
−0.10 to 0.00 cm
Number of Hemispheres
Number of Tracks
0
4000
8000
12000
16000
20000
0
5
10
15
20
25

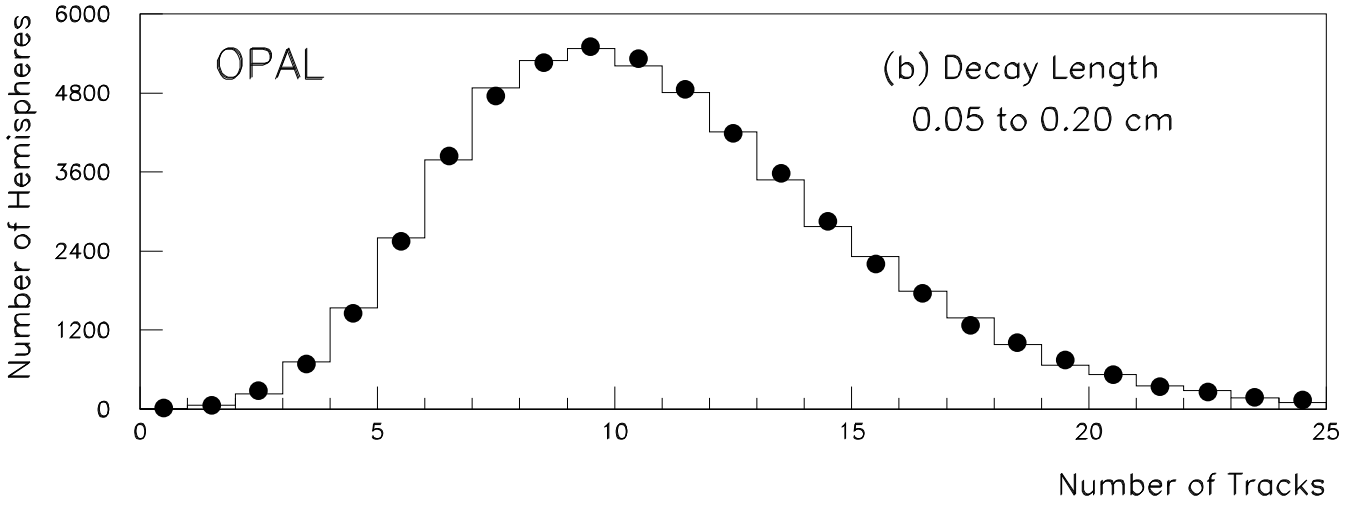
OPAL
(b) Decay Length
0.05 to 0.20 cm
Number of Hemispheres
Number of Tracks
0
1200
2400
3600
4800
6000
0
5
10
15
20
25

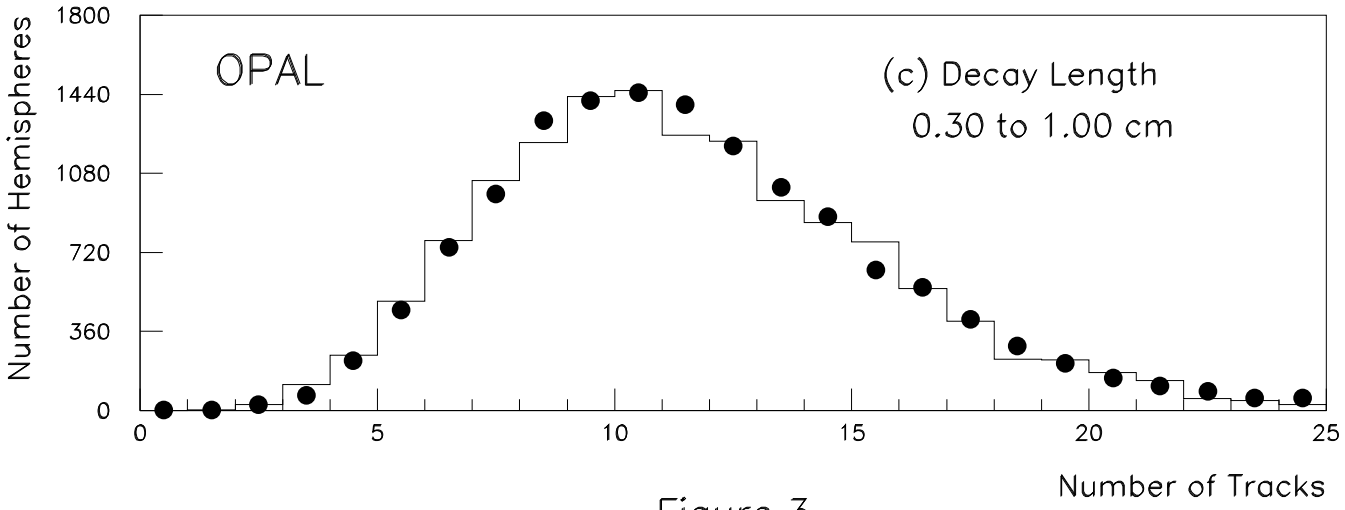
OPAL
(c) Decay Length
0.30 to 1.00 cm
Number of Hemispheres
Number of Tracks
0
360
720
1080
1440
1800
0
5
10
15
20
25

Figure 3

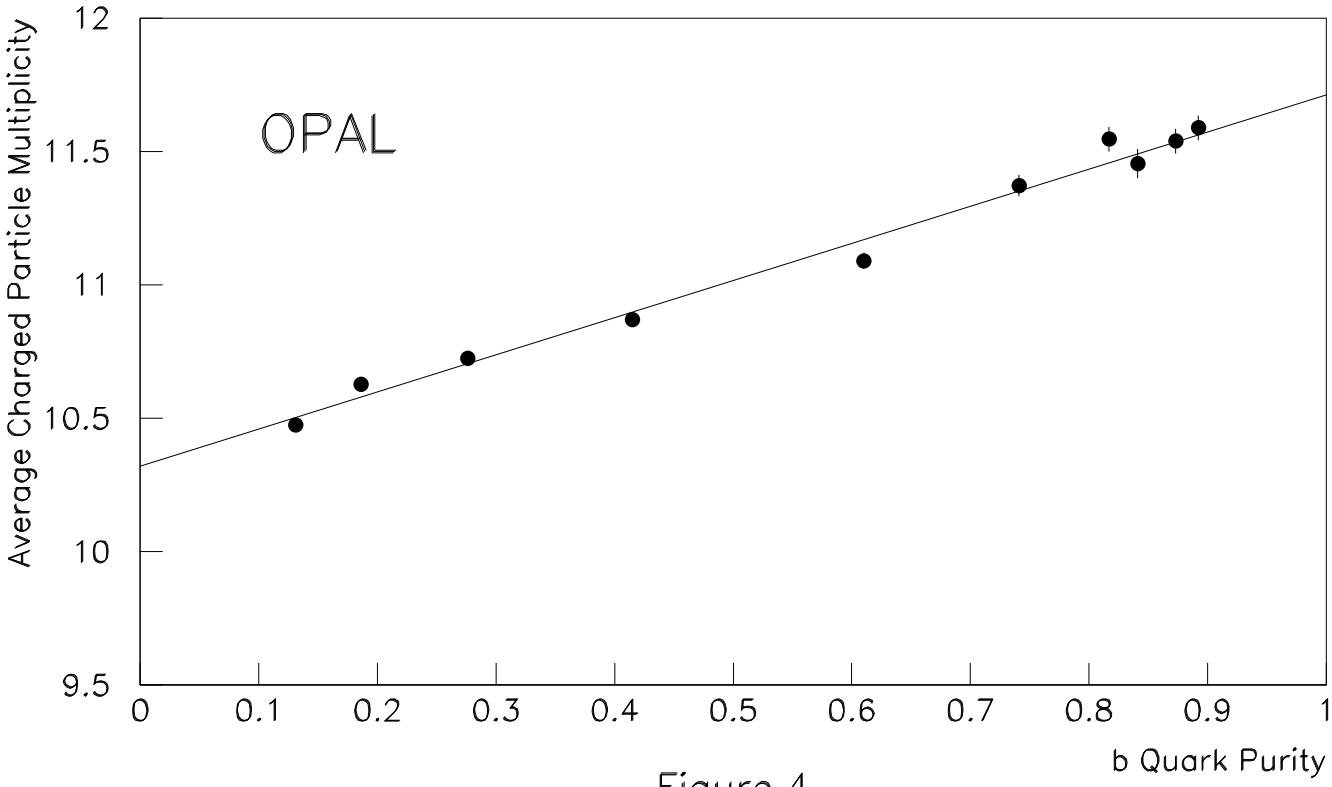
OPAL
Average Charged Particle Multiplicity
b Quark Purity
12
11.5
11
10.5
10
9.5
0
0.1
0.2
0.3
0.4
0.5
0.6
0.7
0.8
0.9
1

Figure 4

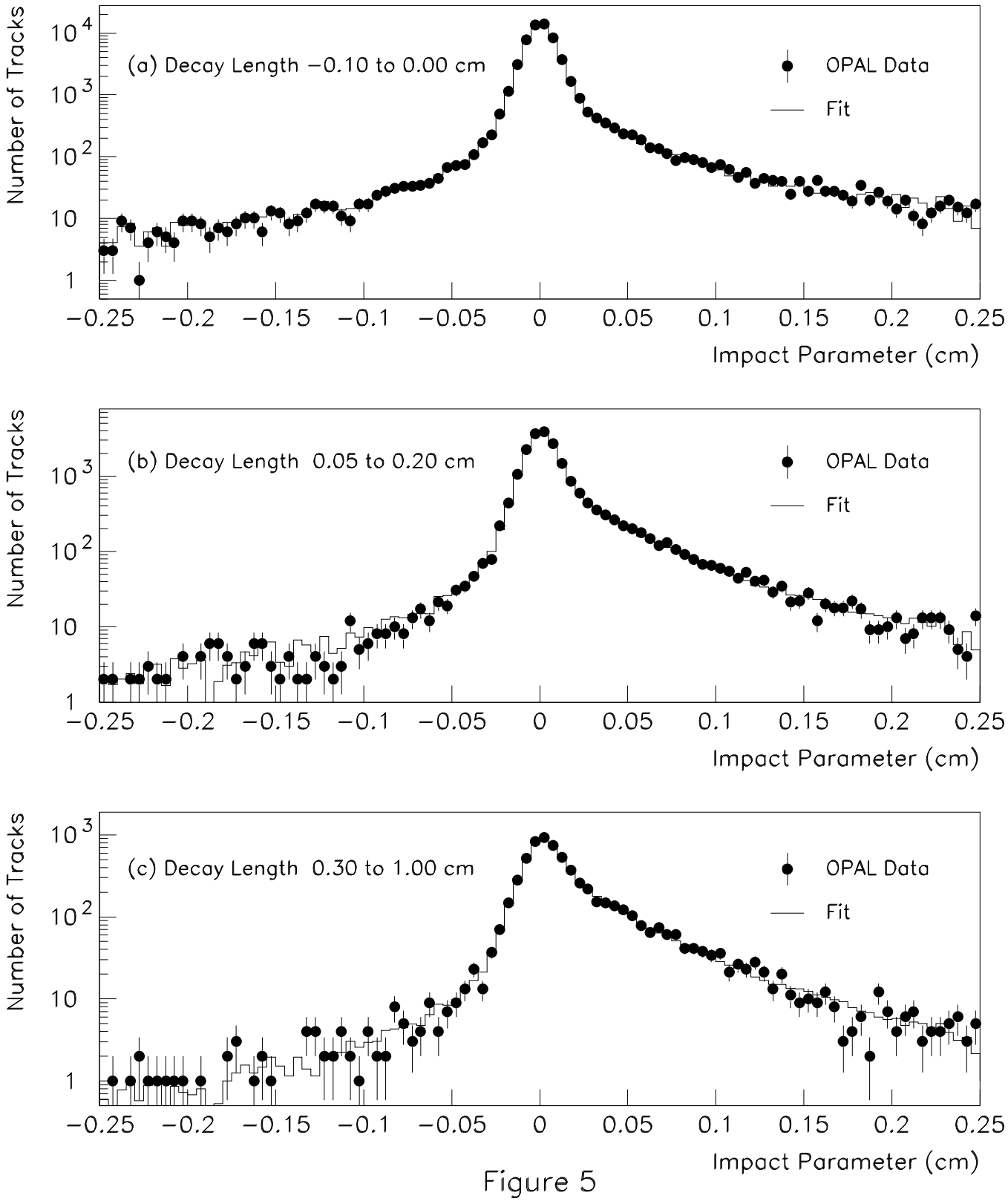
(a) Decay Length −0.10 to 0.00 cm
OPAL Data
Fit
Number of Tracks
Impact Parameter (cm)
(b) Decay Length 0.05 to 0.20 cm
OPAL Data
Fit
Number of Tracks
Impact Parameter (cm)
(c) Decay Length 0.30 to 1.00 cm
OPAL Data
Fit
Number of Tracks
Impact Parameter (cm)

Figure 5

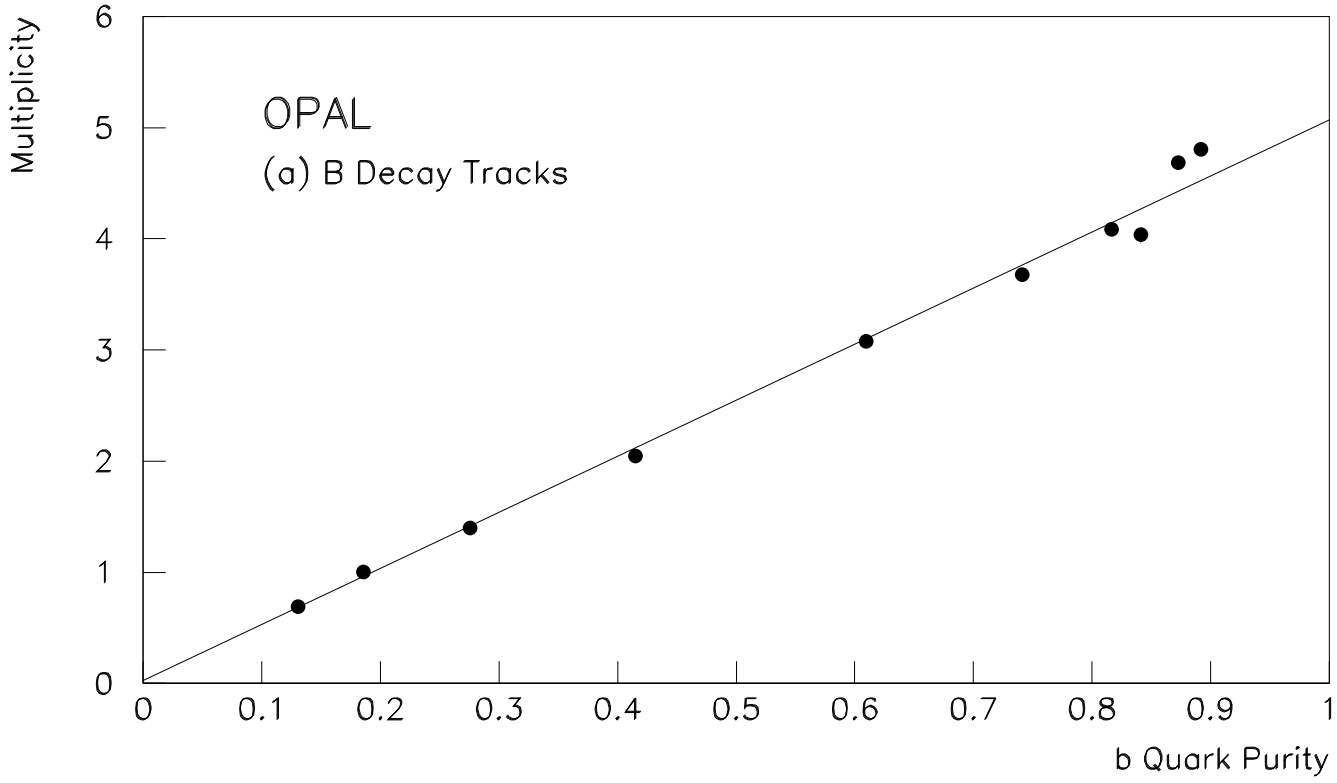
Multiplicity
OPAL
(a) B Decay Tracks
b Quark Purity

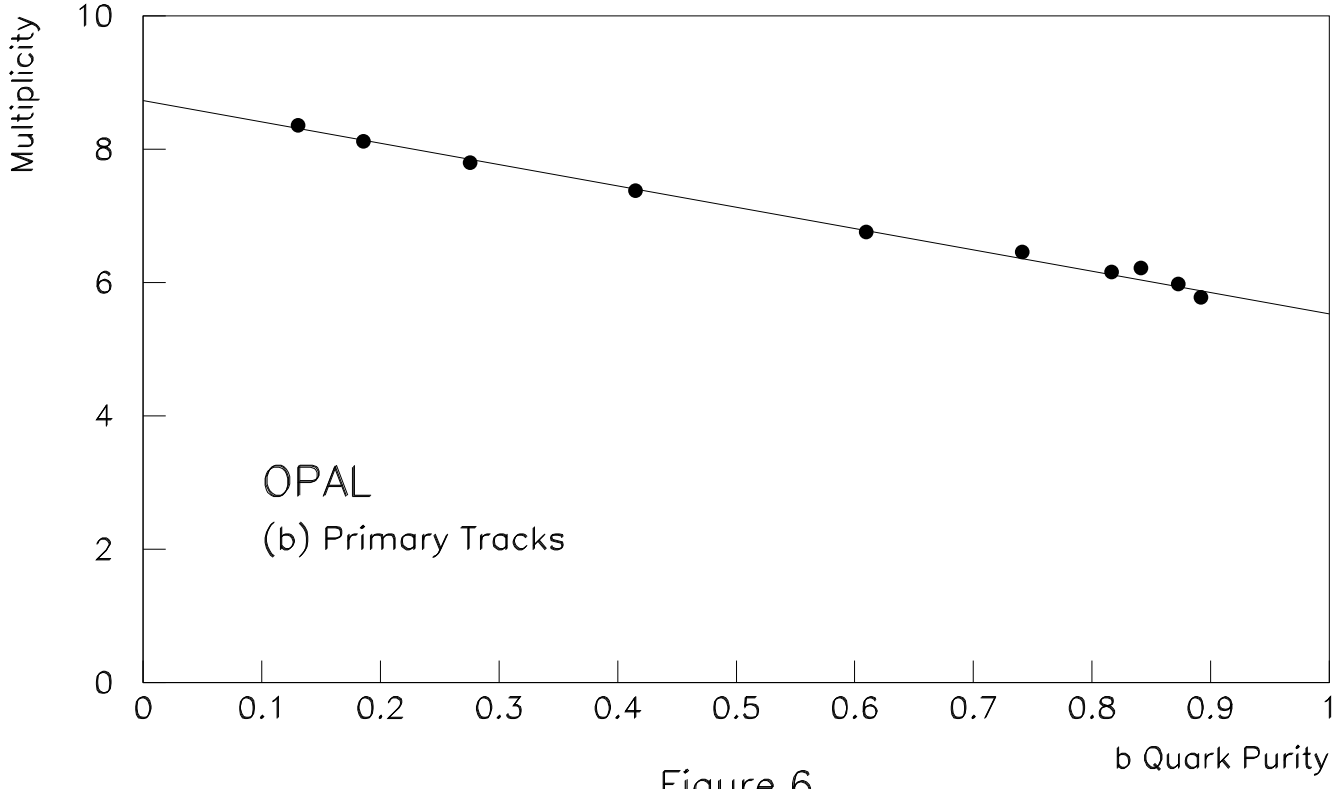
Multiplicity
OPAL
(b) Primary Tracks
b Quark Purity

Figure 6

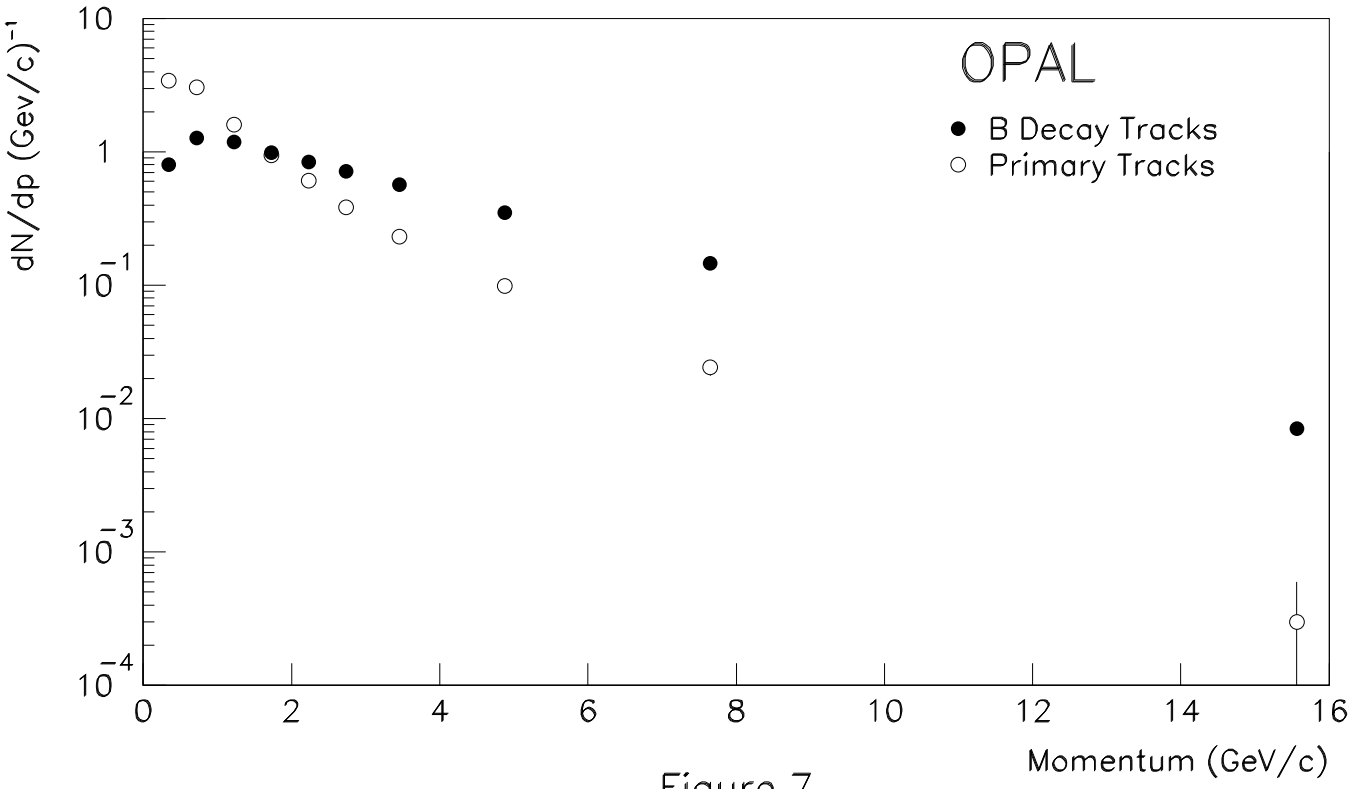

Figure 7

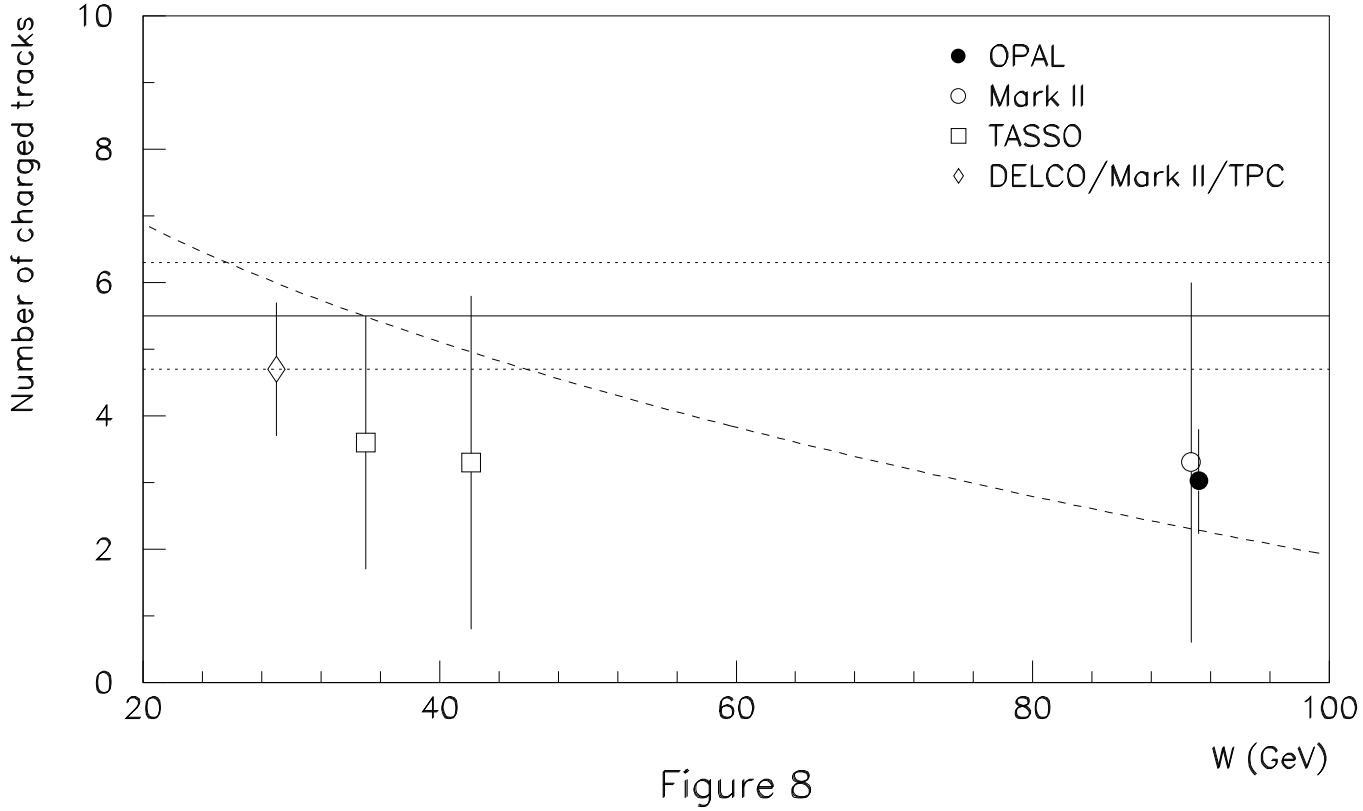

Figure 8